M-2909

J. Chem. Thermodynamics **1993**, 25, 1089–1117

Heat capacities of the wüstites $Fe_{0.9379}O$ and $Fe_{0.9254}O$ at temperatures T from 5 K to 350 K. Thermodynamics of the reaction: xFe(s) + (1/4)Fe_3O_4(s) = $Fe_{0.7500+x}O$(s) = $Fe_{1-y}O$(s) at $T \approx 850$ K, and properties of $Fe_{1-y}O$(s) to T = 1000 K. Thermodynamics of formation of wüstite

Fredrik Grønvold, Svein Stølen,

Department of Chemistry, University of Oslo, Blindern N-0315 Oslo 3, Norway

Pauline Tolmach,[a] and Edgar F. Westrum, Jr.

Department of Chemistry, University of Michigan, Ann Arbor, MI 48109, U.S.A.

(Received 22 February 1993)

Thermodynamic properties of wüstites prepared from iron and iron(III) oxide, have been studied by adiabatic calorimetry. Heat-capacity measurements of metastable $Fe_{0.9379}O$ and $Fe_{0.9254}O$ from T = 5 K to 350 K yielded the following integrated values at T = 298.15 K:

	$\Delta_0^T S_m^\circ$/(J·K^{-1}·mol^{-1})	$\Delta_0^T H_m^\circ$/(J·mol^{-1})
(1/1.9379)$Fe_{0.9379}O$	29.46	4847
(1/1.9254)$Fe_{0.9254}O$	29.21	4821

The wüstites were decomposed to iron and iron(II, III) oxide at $T \approx 800$ K and then recombined in the calorimeter. The enthalpy absorption started at $T \approx 850$ K. It needed increased temperature and several days for completion: up to T = 932 K and 7.1 d total for $Fe_{0.9247}O$, up to T = 898.4 K and 2.1 d for $Fe_{0.9379}O$, and up to T = 948 K and 3.0 d for $Fe_{0.9254}O$. By averaging the results for the two last determinations, the molar enthalpy of the eutectoid formation reaction:

$$0.1817Fe + (1/4)Fe_3O_4 = Fe_{0.9317}O,$$

is $\Delta_r H_m^\circ = (9.04 \pm 0.25)$ kJ·mol^{-1}. The observed eutectoid formation temperature on heating was 854 K on the iron side and 844 K on the magnetite side. In order to delineate the composition range of wüstite at T < 1270 K, thermodynamic functions for FeO and $Fe_{0.90}O$ were estimated and combined with available standard Gibbs free energies of formation for wüstite and the neighboring magnetite phase at T = 1270 K. The resulting eutectoid composition is $Fe_{0.932\pm0.004}O$ and the calculated eutectoid temperature is (847 ± 7) K.

[a] Present address: OLI Systems, American Enterprise Park, 108 American Road, Morris Plains, NJ 07950, U.S.A.

0021–9614/93/091089+29 $08.00/0

1. Introduction

The $Fe_{1-y}O$ phase, wüstite, forms eutectoidally from Fe and Fe_3O_4 (magnetite) at temperature $T \approx 850$ K. It is quenchable and remains metastable at ambient conditions for extended periods. So far, the heat capacity up to ambient temperature has been accurately determined only for a wüstite of composition $Fe_{0.947}O$. We have prepared three more oxygen-rich wüstites and thought it of interest to determine the low-temperature heat capacities of two of them, $Fe_{0.9379}O$ and $Fe_{0.9254}O$, to gain insight into the effect of composition on the thermodynamic properties.

Wüstite slowly reverts to the stable mixture of Fe and Fe_3O_4 at $T < 850$ K. A two-phase mixture with composition equal to that of eutectoid wüstite should thus react at one definite temperature, while mixtures deviating somewhat from that composition should react in part also above the eutectoid temperature. Thus, by heating such mixtures in our adiabatic-shield calorimeter, both the reaction temperature, the reaction entropy, and the eutectoid composition might be derived.

Wüstite is the classical example of a non-stoichiometric phase, and it has been characterized by a variety of physicochemical techniques. The value of X-ray diffraction in determining the extension of the phase field of wüstite—even with use of quenched samples—was demonstrated through the thorough work by Jette and Foote[1,2] in the 1930s. Numerous lattice-constant determinations have been carried out since that time by diffraction techniques employing X-rays and neutrons.[3–15] On combining the X-ray results with density measurements Jette and Foote[1,2] discovered a new type of solid solution, termed subtraction type by Hägg.[16] It is characterized by an increasing number of vacant iron sites in the NaCl-type structure with increasing oxygen content. The neutron-diffraction work by Roth[17] showed that the iron deficiency leads to displacement of iron atoms to tetrahedrally coordinated interstices. Roth saw a one-to-one correspondence between subtraction and displacement of iron atoms, leading to a 2/1 cluster {two octahedral vacancies to one tetrahedral iron, presumably Fe(III)}. Spatial considerations indicate, however, that the other two iron atoms cannot remain at the corners of the cube surrounding Fe(III), because of the unreasonably short nearest-neighbor distance between such centers (Fe–2Fe = 187 pm). They need to be removed in order to stabilize the cluster, which is then of the 4/1 type. This condition implies that a substantial fraction of the formally oxidized iron atoms remain at their octahedral centers. Aggregates of clusters with varying (octahedral vacancy)/(tetrahedral iron) site ratio have been inferred from superstructure-cell characteristics,[6,7,14,18–26] and the existence of three—and more recently six—subphases has been claimed from structural and thermodynamic evidence.[27–36]

The initial theoretical modeling[37,38] suggested that edge-shared cluster aggregates with ratios 6/2 and 8/3 are more stable than corner-shared aggregates with ratios 13/4 and 16/5. Later studies[26,39,42] have stressed the importance of further ratios: 5/2, 10/3, 12/4, 13/5, and 16/7. According to the recent calculations by Press and Ellis[43] the popular 13/4-Koch–Cohen[21]-aggregate cluster is not a serious contender as a stable configuration of extended 4/1 clusters. The 7/2 and 8/3 clusters allow more favorable contact with many surrounding Fe(III) neighbors and

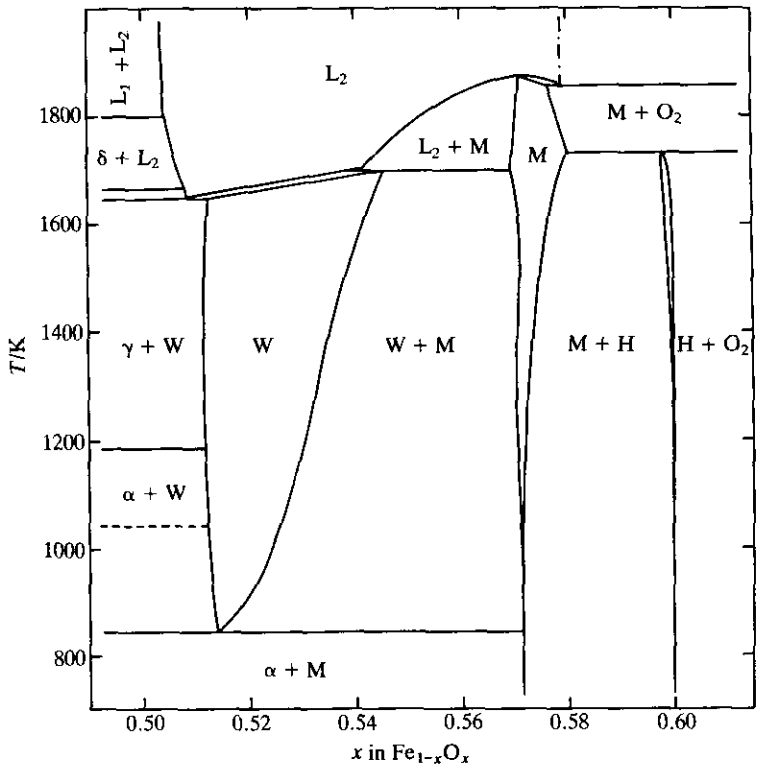

FIGURE 1. Phase diagram of the $Fe_{1-x}O_x$ condensed system in the FeO to Fe_2O_3 region. – – –, Ferro/para-magnetic transition in iron (designated α, γ, and δ); L_1, iron-rich liquid; –·–, $p(O_2)$ = 0.1 MPa over liquid L_2; $Fe_{1-y}O$, wüstite (W); $Fe_{3\pm x}O_4$, magnetite (M); α-Fe_2O_{3-x}, hematite (H).

thus increased stabilization. The presence of cluster aggregates indicates that the residual structural disorder entropy is small.

Below 190 K antiferromagnetic ordering is observed in wüstite.[44,45] It is accompanied by a slight rhombohedral deformation.[46,47]

The thermodynamic characterization of the wüstite phase was advanced considerably through the work by Darken and Gurry.[48] According to the phase diagram presented by them, those revised more recently by other authors[49-53] and the one redrawn here in figure 1, the phase field of the $Fe_{1-y}O$ phase does not extend near the stoichiometric composition $y = 0$, (or $x = \frac{1}{2}$ for $Fe_{1-x}O_x$). On the oxygen-rich side, Darken and Gurry[48] saw increasing solubility of oxygen with temperature. Thus, the retrograde-solubility curve derived by Jette and Foote[1,2] was probably the result of decreasing quenchability of the $Fe_{1-y}O$ phase with increasing oxygen content. The subdivision of the wüstite phase is not shown in figure 1.

The most reliable earlier heat-capacity measurements on wüstite are those for $Fe_{0.947}O$ by Todd and Bonnickson[54] from $T = 52$ K to 298 K and the enthalpy-

increment measurements by Coughlin *et al.*[55] on the same sample over the range $T = 298$ K to 1784 K. These results superseded earlier measurements by Millar[56] and by White,[57] respectively. Later enthalpy-increment results by Vladimirov and Ponomarev[58] over the range $T = 273$ K to 1373 K are too high to be credible, except at the highest temperatures, see below. Thus, the earlier high-temperature heat-capacity results on wüstite were obtained only from drop-calorimetric experiments.

Relative heat-capacity measurements on five $Fe_{1-y}O$ samples in the range $T =$ 140 K to 220 K were reported by Mainard *et al.*[59] They show that the heat-capacity peak due to the transition from antiferro- to para-magnetism in $Fe_{1-y}O$ around $T = 190$ K is greatly reduced, while the peak temperature rises with decreasing iron content from $Fe_{0.944}O$ to $Fe_{0.899}O$. More recently Rogez *et al.*[60] measured enthalpy increments from $T = 299$ K to 1179 K for nine $Fe_{1-y}O$ samples ($0.8835 \leqslant 1-y \leqslant 0.9515$). Despite considerable scatter of the results, the molar enthalpy increment was deduced to increase linearly with composition from about 45.0 $kJ \cdot mol^{-1}$ for $Fe_{0.95}O$ to 46.5 $kJ \cdot mol^{-1}$ for $Fe_{0.88}O$. The former value is 4 per cent lower than that found by Coughlin *et al.*[55] for $Fe_{0.947}O$ over the same temperature region and casts some doubt on the accuracy of the newer results. These measurements are discussed later.

Several descriptions and model calculations of the phase field of wüstite have been based on the wealth of thermodynamic quantities on wüstite and the other iron oxides. The chemical potential of oxygen is well known through the numerous gas-equilibrium studies ($H_2 + \frac{1}{2}O_2 = H_2O$; $CO + \frac{1}{2}O_2 = CO_2$). The partial molar entropy of oxygen has been derived from the temperature dependence of $\Delta_f G^\circ_m$, and more recently in combination with titration-calorimetric results. Further results from e.m.f. studies *etc.* have allowed a detailed description of the formation properties of wüstite to be made as function of composition and temperature.[49, 51, 53, 61–63]

The recent—still unpublished—network evaluation by Haas[64] led to a more oxygen-rich composition of eutectoid wüstite than many other studies. Thus, we have tried to locate the composition of eutectoid wüstite with our calorimeter and to determine the reaction enthalpy and reaction entropy of wüstite from iron and magnetite. The present results have been combined with formation results from wüstite and its neighbor phases at $T = 1270$ K to obtain a consistent thermodynamic description of the wüstite phase field down to the eutectoid decomposition temperature at ambient pressure.

2. Experimental

The wüstites used in this investigation were prepared from iron(III) oxide and iron. The Fe_2O_3 (pro analysi, E. Merck No. 3924) was heated in alumina boats in an electric furnace at $T = 1070$ K until constant mass was attained. This required about 40 h and resulted in a mass loss of $0.0005 \cdot m$. According to the manufacturer's analysis the mass fractions of impurities are: Cl^-, $1 \cdot 10^{-4}$; SO_4^{2-}, $1 \cdot 10^{-4}$; N, Pb, Cu, Mg, Mn, Ni, Zn, $5 \cdot 10^{-5}$; insoluble in HCl, $1 \cdot 10^{-4}$. A spectrographic analysis revealed in addition the presence of mass fraction $50 \cdot 10^{-6}$ of SiO_2.

TABLE 1. X-ray powder-diffraction results for the iron oxides after successive heat treatments: f, furnace cooled; q, quenched in (ice + brine)

Nominal comp.	T/K	Time	Cool	Phases
$Fe_{0.9493}O$	1270	2 d	f	Fe_3O_4; $Fe_{1-y}O$; Fe
	800	7 d	f	Fe_3O_4; Fe; some ≈FeO, a = 432.7 pm
	770	180 d	f	Fe_3O_4; Fe
	870	7 d	q	$Fe_{1-y}O$, a = 430.4 pm
	1120	2 d	q	$Fe_{1-y}O$, a = 430.8 pm
$Fe_{0.9455}O$	1270	2 d	f	Fe_3O_4; ≈FeO, a = 432.8 pm; Fe; $Fe_{1-y}O$, a = 430.0 pm
	1270	2 d	q	$Fe_{1-y}O$, a = 430.1 pm
	700	7 d	f	Fe_3O_4; Fe; some ≈FeO, a = 433 pm
	770	240 d	f	Fe_3O_4; Fe
	870	4 h	q	$Fe_{1-y}O$, a = 430 pm; some ≈FeO, a = 433 pm
	870	1 d	q	$Fe_{1-y}O$, a = 430.2 pm
	1270	2 d	q	$Fe_{1-y}O$, a = 430.1 pm
$Fe_{0.9300}O$	1270	2 d	f	Fe_3O_4; Fe; $Fe_{1-y}O$
	770	70 d	f	Fe_3O_4; Fe; some $Fe_{1-x}O$, a = 430 pm; trace ≈FeO, a = 433 pm
	770	100 d	f	Fe_3O_4; Fe; trace $Fe_{1-y}O$, a = 430 pm
	790	120 d	f	Fe_3O_4; Fe
	870	1 d	q	$Fe_{1-y}O$, a = 429.8 pm
	920	1 d	q	$Fe_{1-y}O$, a = 429.9 pm
	1120	1 d	q	$Fe_{1-y}O$, a = 429.8 pm

A small part of the sample was reduced to iron with dry hydrogen gas at T = 1120 K until the mass ratio $m(Fe_2O_3)/m(Fe)$ was (1.4295 ± 0.0002); theoretical, 1.4297. Mixtures of this Fe and the Fe_2O_3 with nominal mole ratios $n(Fe)/n(O)$ 0.9493, 0.9455, and 0.9300 were heated in evacuated and sealed vitreous silica tubes at T = 1270 K for 2 d and furnace cooled. Two batches of mass about 70 g each were crushed and mixed. The major part of each sample was placed in a silica glass tube, and smaller fractions in additional tubes. The mixtures were heated in the temperature range 770 K to 800 K for as long as 290 d. The smaller tubes were removed from the furnace at intervals in order to check the decomposition process by X-ray diffraction, see table 1.

Room temperature X-ray photographs were taken in a Philips diffractometer with Cr $K\alpha_1$ radiation and Si as an internal calibration substance, a(293 K) = 543.1065 pm.[65] In nominal $Fe_{0.9493}O$ some metastable wüstite with approximately stoichiometric composition, ≈FeO, was observed after 7 d tempering at T = 800 K. It was completely absent after 180 d tempering at T = 770 K. In $Fe_{0.9455}O$ four solid phases (Fe, ≈FeO, $Fe_{1-y}O$, and Fe_3O_4) were present after 7 d tempering at T = 770 K also. In $Fe_{0.9300}O$ a trace of $Fe_{1-y}O$ was still present after a total tempering time of 170 d at T = 770 K. The main portion of the sample was then transferred to the calorimetric ampoules and heated at T = 790 K for 120 d more. After the thermal measurements on nominal $Fe_{0.9455}O$ in the range T = 800 K to 1000 K the ampoule was heated at T = 1070 K (1 d), at 970 K (2 h), and then quenched in (ice + brine) before measurements were made in the T = 300 K to

TABLE 2. Relative mass ratio w_r upon oxidation—and reduction—of the iron oxides, and the resulting composition; mass fraction W of SiO_2

Nominal oxide composition	w_r uncorr.	w_r corr. for SiO_2	$n(Fe)/n(O)$	Real oxide composition	$10^2 \cdot W$
$Fe_{0.9493}O$					
ox	1.09646	1.09654	0.9428		
ox	1.09640	1.09649	0.9426	$Fe_{0.9427}O$	0.09
ox	1.09644	1.09653	0.9428		
$Fe_{0.9455}O$					
ox	1.09498	1.09547	0.9389		
ox	1.09457	1.09508	0.9374		
ox	1.09459	1.09508	0.9374	$Fe_{0.9379}O$	0.52
red	0.7678	0.7660	0.9378		
$Fe_{0.9300}O$					
ox	1.09164	1.09181	0.9256		
ox	1.09147	1.09168	0.9252	$Fe_{0.9254}O$	0.23

400 K region. This ampoule and the one with nominal $Fe_{0.9300}O$ were then opened and the contents of each transferred to four 8 mm i.d. silica glass tubes. After evacuation and sealing they were heated at $T = 1070$ K for 1 d and quenched in (ice + brine) before measurements in the $T = 5$ K to 350 K region.

The oxygen content of the calorimetric samples was determined by oxidation of samples of mass 10 g to 15 g at $T = 1070$ K in air to constant mass in platinum crucibles or alumina boats. Nominal $Fe_{0.9455}O$ was also reduced with dry hydrogen gas. The latter process went very slowly and was finally complete after successive heatings at $T = 870$ K, 970 K, and 1120 K for 6 d, 2 d, and 1 d, respectively. The oxidation and reduction experiments did not result in coinciding compositions for nominal $Fe_{0.9455}O$, and indicated the presence of some non-reducible material. Part of the reduced product was kindly analyzed for oxygen and silicon by Sandvik Hard Materials, Sweden, through the courtesy of Dr Bjørn Uhrenius. It contained (0.31 ± 0.01) mass per cent of O and 0.32 mass per cent of Si, which corresponds closely to the presence of 0.52 mass per cent of SiO_2 in the wüstite. This impurity probably arose from the reaction of the oxide with the silica glass wall, the flaking off of some devitrified silica, and the introduction of small glass fragments during opening of the tubes. In keeping with this, the nominal $Fe_{0.9455}O$ sample was found to contain 0.6 mass per cent of material insoluble in hydrochloric acid, mainly SiO_2. For nominal $Fe_{0.9493}O$ the insoluble residue was 0.09 mass per cent and for nominal $Fe_{0.9300}O$ it averaged 0.23 mass per cent (mainly SiO_2).

The results of the (oxidation and reduction) determinations of the oxygen content of the samples are summarized in table 2. The increase in oxygen content from the weighed-in composition is presumably due to slight oxidation of finely precipitated iron in the crushing and resealing process.

The cryogenic calorimetric measurements were made in the Mark XIII cryostat described previously,[66] using intermittent-heating adiabatic equilibrium methods. The programming, logging, and calorimetry were computerized as described

elsewhere.[67] A gold-plated copper calorimeter (designated W-139) was loaded separately with masses 67.914 g of $Fe_{0.9379}O$ and 54.764 g of $Fe_{0.9254}O$. The buoyancy correction was calculated on the assumed density of 5.68 $g \cdot cm^{-3}$. Following evacuation, purified helium at 0.4 kPa pressure was added to enhance thermal equilibration. The calorimeter was then sealed in a vacuum chamber *via* a monel screw cap, which pressed a gold gasket against the circular knife edge on the stainless-steel neck of the calorimeter. All measurements of mass, resistance, potential, and time were referred to standardizations and calibrations performed at the former U.S. National Bureau of Standards, (now the National Institute of Standards and Technology), the U.K. National Physical Laboratory, and/or the Norwegian National Measurement Service.

The higher-temperature calorimetric apparatus and measuring technique have been described previously.[68] The calorimeter was intermittently heated, and surrounded by electrically heated and electronically controlled adiabatic shields. The masses used in the experiments were about 90 g, with one exception: 73 g for $Fe_{0.9379}O$ in Series VI. They were enclosed in evacuated and sealed vitreous silica tubes of about 50 cm^3 volume, tightly fitted into the silver calorimeter. A central well in the tube served for the heater and platinum resistance thermometer. The thermometer was calibrated locally, at the ice, steam, tin, zinc, and antimony points. Temperatures are judged to correspond with IPTS-68 to within 0.08 K up to the antimony point, and within 0.2 K at 1000 K.

The heat capacity of each empty calorimeter was determined in a separate series of experiments. It was, for the low-temperature calorimetric experiments, about 30 per cent of the total below 30 K decreasing to about 15 per cent above 200 K in the case of $Fe_{0.9379}O$, and from about (35 to 20) per cent for $Fe_{0.9254}O$. For the higher-temperature experiments the heat capacity of the empty calorimeter was about 50 per cent of the total, except in the transitional region, in which a reaction occurred, forming wüstite from Fe and Fe_3O_4.

3. Results and discussion

The results of the molar heat-capacity determinations are presented in table 3 in chronological order for $Fe_{0.9427}O$, $Fe_{0.9379}O$, and $Fe_{0.9254}O$. The approximate temperature increments used in the determinations can usually be inferred from the adjacent mean temperatures given in the table. The thermal history of the samples and the relation of the measurements to UofM and UofO are recorded in table 4. The $Fe_{0.9379}O$ was subjected to more detailed study, both in quenched form as wüstite, and in decomposed form as $\{0.1879Fe + (1/4)Fe_3O_4\}$. Corrections for the presence of SiO_2 were applied.

MOLAR HEAT CAPACITIES AND THERMODYNAMIC FUNCTIONS FOR METASTABLE WÜSTITES UP TO $T = 850$ K AND OF STABLE WÜSTITES AT $T > 850$ K

The molar heat-capacity results for quenched $Fe_{0.9379}O$ are shown over the range $T = 5$ K to 300 K in figure 2. A small, blunt maximum is observed at $T = 189.5$ K. It

TABLE 3. Molar heat capacities of $Fe_{0.9427}O$, $Fe_{0.9379}O$, and $Fe_{0.9254}O$, $R = 8.3145\ J \cdot K^{-1} \cdot mol^{-1}$

T/K	$C_{p,m}/R$	T/K	$C_{p,m}/R$	T/K	$C_{p,m}/R$	T/K	$C_{p,m}/R$	T/K	$C_{p,m}/R$	T/K	$C_{p,m}/R$
					$M(Fe_{0.9427}O) = 68.646\ g \cdot mol^{-1}$						
Series I		853.76	348.67	858.79	89.69	885.84	6.898	912.82	6.884	938.37	6.721
844.61	10.282	854.41	184.01	871.08	11.195	899.46	6.937	925.52	6.905	951.47	6.744
850.66	9.787									964.58	6.753
					$M(Fe_{0.9379}O) = 68.378\ g \cdot mol^{-1}$						
Series I		903.61	6.589	16.48	0.0349	112.35	3.345	279.90	5.811	193.67	5.633
303.34	5.181	916.35	6.643	18.00	0.0458	118.31	3.592	286.14	5.842	195.78	5.569
311.31	5.273	929.07	6.715	19.54	0.0580	124.29	3.829	292.37	5.857	198.39	5.567
319.62	5.273	941.67	6.660	21.25	0.0757	130.28	4.069	298.60	5.871	201.51	5.548
327.91	5.333	954.48	6.675	23.10	0.0989	136.30	4.386	304.83	5.893	204.63	5.549
336.16	5.393	967.37	6.663	25.00	0.1250	142.36	4.551	311.06	5.913	207.76	5.558
344.37	5.470	980.34	6.657	27.18	0.1608	148.42	4.792	317.28	5.920	Series VI	
352.55	5.527	993.45	6.589	29.62	0.2071	154.50	5.047	323.50	5.938	301.88	5.855
360.70	5.589	Series III		32.09	0.2611	160.58	5.279	329.71	5.949	312.03	5.920
368.83	5.629	301.96	5.863	34.61	0.3217	166.68	5.510	335.90	5.989	322.14	5.949
376.93	5.699	312.87	5.883	37.41	0.3994	172.83	5.657	342.10	5.990	332.23	5.990
385.01	5.750	323.65	5.962	40.48	0.4884	179.05	5.749	347.81	6.008	342.31	6.039
393.07	5.795	334.38	5.979	43.60	0.5869	185.33	5.778	Series V		352.43	6.086
401.11	5.830	345.14	6.023	46.78	0.6921	191.69	5.743	133.75	4.207	362.59	6.109
409.14	5.848	355.86	6.045	50.37	0.8209	198.13	5.564	139.03	4.420	372.76	6.088
417.16	5.962	366.54	6.062	54.38	0.9656	204.55	5.545	145.00	4.656	382.95	6.093
425.16	5.984	377.18	6.086	58.43	1.119	210.89	5.560	150.97	4.895	393.15	6.135
Series II		387.81	6.097	62.54	1.280	217.21	5.583	156.95	5.131	403.34	6.153
791.94	8.758	398.41	6.112	67.00	1.459	223.53	5.611	162.93	5.383	413.55	6.162
808.34	9.020	Series IV		71.76	1.647	229.85	5.631	168.94	5.511	423.69	6.159
824.32	9.383	7.01	0.0068	76.53	1.847	236.17	5.658	175.03	5.706	433.78	6.163
840.05	10.026	9.06	0.0066	81.33	2.051	242.50	5.689	179.63	5.756	443.88	6.195
851.67	83.03	9.91	0.0080	86.18	2.269	248.77	5.704	182.74	5.754	454.02	6.225
862.94	11.673	11.06	0.0110	91.07	2.465	255.00	5.731	185.33	5.762	464.73	6.265
871.40	11.822	12.31	0.0150	96.00	2.666	261.23	5.753	187.41	5.779	475.32	5.376
880.90	7.892	13.56	0.0205	100.96	2.876	267.46	5.774	189.48	5.789	486.94	3.856
892.57	7.351	14.97	0.0265	106.41	3.099	273.69	5.793	191.57	5.751		
					$M(Fe_{0.9254}O) = 67.680\ g \cdot mol^{-1}$						
Series I		10.21	0.0084	43.63	0.5676	115.35	3.428	178.00	5.402	252.81	5.776
815.42	9.153	11.44	0.0120	45.51	0.6500	120.29	3.609	182.10	5.508	258.03	5.826
839.87	9.984	12.59	0.0137	47.61	0.7175	125.27	3.810	185.17	5.580	263.23	5.819
853.22	58.116	13.98	0.0220	49.86	0.7989	130.27	3.980	188.86	5.591	268.44	5.806
864.84	20.458	15.32	0.0290	52.21	0.8828	135.27	4.176	191.53	5.585	273.64	5.848
871.62	21.950	16.67	0.0368	54.68	0.9742	143.13	4.410	Series V		278.80	5.870
880.25	10.245	18.08	0.0479	57.26	1.0660	148.06	4.558	186.76	5.558	284.00	5.896
891.72	7.714	19.64	0.0603	60.01	1.1520	153.11	4.738	189.81	5.619	289.22	5.876
904.13	7.279	21.20	0.0774	62.84	1.2773	158.16	4.870	192.91	5.635	294.41	5.917
916.61	7.161	22.79	0.0955	65.83	1.4056	163.23	5.003	196.05	5.523	299.58	6.020
929.22	7.131	24.39	0.1176	68.96	1.5445	168.29	5.165	199.18	5.501	304.85	5.964
941.94	6.809	26.06	0.1418	72.30	1.664	173.36	5.275	202.29	5.555	310.08	5.937
957.08	6.615	27.76	0.1750	75.78	1.813	178.43	5.419	206.43	5.555	315.28	5.950
972.31	6.601	29.49	0.2069	79.49	1.924	182.26	5.539	211.62	5.575	320.46	5.962
985.69	6.615	31.26	0.2451	83.28	2.111	184.83	5.581	216.81	5.596	325.53	5.909
999.10	6.654	33.03	0.2874	87.28	2.304	Series III		221.80	5.627	330.64	5.982
Series II		34.72	0.3276	91.52	2.471	198.39	5.667	227.01	5.652	335.79	6.002
5.94	0.0023	36.37	0.3726	95.99	2.644	201.51	5.548	232.25	5.643	340.95	6.065
7.21	0.0033	38.05	0.4159	100.67	2.841	Series IV		237.30	5.662	346.71	6.061
8.24	0.0045	39.82	0.4685	105.53	3.035	167.78	5.145	242.39	5.790		
9.23	0.0050	41.70	0.5068	110.43	3.234	172.87	5.334	247.58	5.784		

TABLE 4. Thermal history

Series	Previous treatment	Place
	$Fe_{0.9427}O$	
I	*Reacted at* $T = 1270$ K *for* 2 d, *tempered at* 770 K *for* 180 d, *cooled with* furnace. Transferred to calorimetric ampoule, tempered at 770 K for 7 d, heated to 841 K overnight	*Oslo*
	$Fe_{0.9379}O$	
I	Reacted at $T = 1270$ K for 2 d. Transferred to calorimetric ampoule, tempered at 770 K for 240 d, cooled with furnace	Oslo
II	Heated at $T = 780$ K for 2 d	Oslo
III	Cooled with furnace from $T = 987$ K, transferred to 4 small tubes, heated at 1070 K for 2 d, down to 970 K (2 h) and quenched in (ice + brine)	Oslo
IV	Cooled from ambient T to 5 K during 24 h	Ann Arbor
V	Cooled from $T = 350$ K to 138 K during 24 h	Ann Arbor
VI	Kept at ambient T	Oslo
	$Fe_{0.9254}O$	
I	Reacted at $T = 1270$ K for 2 d and tempered at 770 K for 170 d. Transferred to calorimetric ampoule, tempered at 790 K for 120 d, cooled with furnace, and heated in calorimeter to 777 K overnight	Oslo
II	Cooled from $T = 1006$ K in calorimeter, transferred to 4 small tubes, heated to 1070 K for 2 d, down to 970 K (2 d) and quenched in (ice + brine)	Oslo
	Cooled from ambient T to 5 K during 18 h	Ann Arbor
III	*A.c. bridge problems*	*Ann Arbor*
IV	Cooled from $T = 227$ K to 124 K during 16 h	Ann Arbor
V	Cooled from $T = 228$ K to 164 K during 7.5 h	Ann Arbor

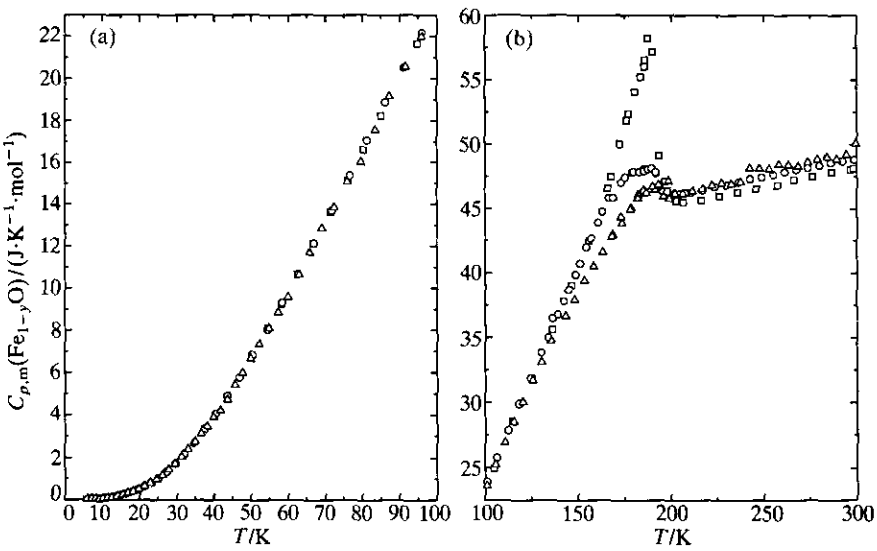

FIGURE 2. Molar heat capacities of quenched wüstites at temperatures from 5 K to 300 K. △, $Fe_{0.9254}O$ present results; ○, $Fe_{0.9379}O$ present results; □, $Fe_{0.947}O$ Todd and Bonnickson.[54]

TABLE 5. Thermodynamic properties of $Fe_{0.9379}O$ and $Fe_{0.9254}O$, $R = 8.3145\ J \cdot K^{-1} \cdot mol^{-1}$

$\frac{T}{K}$	$\frac{C_{p,m}}{R}$	$\frac{\Delta_0^T H_m^\circ}{R \cdot K}$	$\frac{\Delta_0^T S_m^\circ}{R}$	$\frac{\Phi_m^\circ}{R}$	$\frac{T}{K}$	$\frac{C_{p,m}}{R}$	$\frac{\Delta_0^T H_m^\circ}{R \cdot K}$	$\frac{\Delta_0^T S_m^\circ}{R}$	$\frac{\Phi_m^\circ}{R}$
				$M(Fe_{0.9379}O) = 68.378\ g \cdot mol^{-1}$					
5	0.001	0.001	0.000	0.000	230	5.637	737.6	5.371	2.165
10	0.008	0.021	0.003	0.001	240	5.673	794.1	5.612	2.303
15	0.027	0.103	0.009	0.002	250	5.710	851.0	5.844	2.440
20	0.063	0.320	0.021	0.005	260	5.747	908.3	6.069	2.576
25	0.124	0.776	0.042	0.010	270	5.783	966.0	6.287	2.709
30	0.215	1.611	0.072	0.018	280	5.817	1024.0	6.498	2.841
35	0.334	2.971	0.113	0.029	290	5.849	1082.3	6.702	2.970
40	0.474	4.983	0.167	0.042	298.15	5.870	1130.1	6.865	3.075
45	0.632	7.742	0.232	0.060	300	5.877	1141.0	6.901	3.098
50	0.806	11.330	0.307	0.081	350	6.025	1438.7	7.819	3.708
60	1.179	21.242	0.487	0.133	400	6.131	1742.8	8.631	4.274
70	1.581	35.026	0.699	0.198	450	6.213	2051.4	9.358	4.799
75	1.770	43.392	0.814	0.235	500	6.279	2363.8	10.016	5.288
80	1.999	52.81	0.935	0.275	550	6.336	2679.2	10.617	5.746
90	2.424	74.98	1.196	0.363	600	6.386	2997.3	11.171	6.175
100	2.828	101.23	1.472	0.460	650	6.432	3317.7	11.684	6.580
110	3.251	131.61	1.761	0.565	700	6.474	3640.4	12.162	6.961
120	3.668	166.22	2.062	0.677	750	6.513	3965.1	12.610	7.323
130	4.066	204.91	2.372	0.796	800	6.550	4291.6	13.031	7.667
140	4.463	247.54	2.688	0.919	850	6.586	4620.1	13.430	7.994
150	4.868	294.19	3.009	1.048	900	6.621	4950.3	13.807	8.307
160	5.258	344.85	3.336	1.181	950	6.655	5282.2	14.166	8.606
170	5.582	399.13	3.665	1.317	1000	6.688	5615.7	14.508	8.892
180	5.772	456.05	3.990	1.457	(1050	6.726	5949.9	14.834	9.167)
190	5.759	513.8	4.303	1.598	(1100	6.767	6287.2	15.148	9.432)
200	5.553	570.1	4.592	1.741	(1150	6.811	6626.6	15.449	9.687)
210	5.557	625.6	4.862	1.883	(1200	6.859	6968.3	15.740	9.933)
220	5.598	681.4	5.122	2.025	(1250	6.912	7312.6	16.020	10.171)
				$M(Fe_{0.9254}O) = 67.680\ g \cdot mol^{-1}$					
5	0.001	0.001	0.000	0.000	240	5.728	777.3	5.499	2.260
10	0.008	0.020	0.003	0.001	250	5.772	834.8	5.733	2.394
15	0.026	0.099	0.009	0.002	260	5.810	892.7	5.960	2.527
20	0.064	0.314	0.021	0.005	270	5.844	950.9	6.180	2.658
25	0.128	0.779	0.041	0.010	280	5.872	1009.5	6.393	2.788
30	0.220	1.637	0.072	0.018	290	5.897	1068.4	6.600	2.916
35	0.334	3.014	0.115	0.029	298.15	5.916	1116.5	6.764	3.019
40	0.463	4.998	0.167	0.043	300	5.920	1127.5	6.800	3.042
45	0.616	7.684	0.231	0.060	325	5.978	1276.1	7.276	3.350
50	0.799	11.214	0.305	0.081	350	6.075	1426.7	7.722	3.646
60	1.160	21.057	0.483	0.132	400	6.138	1731.1	8.535	4.207
70	1.576	34.754	0.694	0.197	450	6.193	2039.2	9.261	4.729
80	1.999	52.57	0.931	0.274	500	6.248	2350.2	9.916	5.215
90	2.405	74.61	1.190	0.361	550	6.296	2663.9	10.514	5.670
100	2.802	100.64	1.464	0.457	600	6.339	2979.8	11.064	6.097
110	3.210	130.70	1.750	0.562	650	6.380	3297.8	11.573	6.499
120	3.615	164.84	2.047	0.673	700	6.418	3617.8	12.047	6.878
130	3.988	202.89	2.351	0.790	750	6.455	3939.7	12.491	7.238
140	4.315	244.44	2.659	0.913	800	6.492	4263.4	12.910	7.579
150	4.614	289.10	2.967	1.040	850	6.528	4588.9	13.303	7.905
160	4.914	336.73	3.274	1.170	900	6.564	4916.2	13.678	8.215
170	5.219	387.40	3.581	1.302	950	6.599	5245.3	14.034	8.512
180	5.478	440.96	3.887	1.438	1000	6.635	5576.2	14.373	8.797

TABLE 5—*continued*

$\frac{T}{K}$	$\frac{C_{p,m}}{R}$	$\frac{\Delta_0^T H_m^\circ}{R \cdot K}$	$\frac{\Delta_0^T S_m^\circ}{R}$	$\frac{\Phi_m^\circ}{R}$	$\frac{T}{K}$	$\frac{C_{p,m}}{R}$	$\frac{\Delta_0^T H_m^\circ}{R \cdot K}$	$\frac{\Delta_0^T S_m^\circ}{R}$	$\frac{\Phi_m^\circ}{R}$
190	5.590	496.46	4.187	1.574	(1050	6.677	5906.2	14.695	9.070)
200	5.530	552.2	4.473	1.712	(1100	6.720	6241.1	15.007	9.333)
210	5.575	607.7	4.744	1.850	(1150	6.766	6578.2	15.306	9.586)
220	5.628	663.7	5.004	1.988	(1200	6.814	6917.7	15.595	9.831)
230	5.680	720.2	5.256	2.124	(1250	6.865	7259.7	15.875	10.067)

differs considerably from that obtained for a slightly more iron-rich sample, $Fe_{0.947}O$ by Todd and Bonnickson,[54] also shown in figure 2(b), with its high and sharp maximum at $T = 188.5$ K. The marked composition dependence was known already from the work by Mainard *et al.*,[59] but only on a relative scale. The measurements on the metastable wüstite $Fe_{0.9379}O$ could be continued up to $T \approx 450$ K, where the beginning disproportionation of wüstite to $\approx$FeO and Fe_3O_4 caused a positive increasing drift rate of the calorimeter from one energy input to the next.

The experimental molar heat capacities for the low- and high-temperature series were fitted to polynomials by the method of least squares. The fitting, and especially the joins between the fitted segments were checked for continuity by inspection of plots of $(dC_{p,m}/dT)$ against T. The polynomials were then integrated by Simpson's rule, to yield values of the molar thermodynamic functions at selected temperatures as presented in table 5. Within the transition region the molar heat-capacity values were read from large-scale plots and the molar thermodynamic functions were calculated by integration of the curves. At the lowest temperatures the molar heat capacities were smoothed with the aid of a plot of $C_{p,m}/T$ against T^2, and the functions were evaluated from the extrapolation, which yielded $\gamma = 0$ (disregarding the lowest point for $Fe_{0.9379}O$).

Molar function values in the region $T = 450$ K to 900 K were interpolated on the assumption that no transition occurs for metastable $Fe_{0.9379}O$, in keeping with Coughlin *et al.*'s[55] findings for $Fe_{0.947}O$. In this interpolation the results from $T = 278.90$ K to 454.02 K and from 903.61 K to 993.45 K were fitted with the following 4-parameter equation:

$$C_{p,m}/(J \cdot K^{-1} \cdot mol^{-1}) = 51.129 + 4.85282 \cdot 10^{-3}(T/K) - 334.9089 \cdot 10^{3}(K/T)^2 - 40.433488 \cdot 10^{-12}(T/K)^3.$$

The resulting curve is shown in figure 3 together with those from the equation by Coughlin *et al.*[55] and by Vladimirov and Ponomarev.[58] The latter is not exactly comparable as it refers to FeO. The results derived for eutectoid wüstite $Fe_{0.9345}O$ by Vallet and Carel[34] show a sharp maximum in heat capacity at $T = 1045$ K and a discontinuity at 1180 K. No pre-transitional rise was observed for $Fe_{0.9379}O$ up to $T = 1000$ K, and it seems to us that these results by Vallet and Raccah[34] are erroneously reflecting the heat-capacity behavior of iron. Integrated thermodynamic functions from the above equation are listed in table 5.

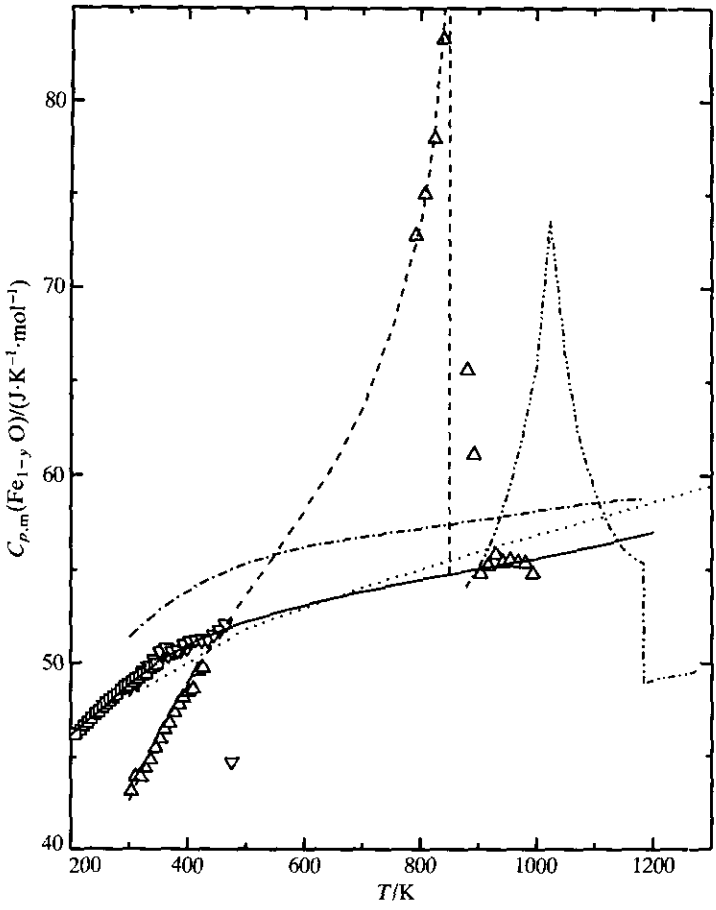

FIGURE 3. Molar heat capacity of $Fe_{0.9379}O$. □, UofM results on quenched wüstite; ▽, UofO results on quenched wüstite; △, UofO results on decomposed wüstite up to $T = 850$ K and of recombining wüstite above; ———, present equation for the wüstite; — — —, present equation for the decomposed wüstite; ···, heat-capacity equation for wüstite ($Fe_{0.947}O$) by Coughlin *et al.*;[55] —·—, equation for FeO by Vladimirov and Ponomarev;[58] —···—, results by Vallet and Carel[34] for eutectoid wüstite $Fe_{0.9345}O$.

The molar heat-capacity results for $Fe_{0.9254}O$ over the region $T = 5$ K to 300 K are also shown in figure 2. Here the peak is at about $T = 193$ K, and even less pronounced, which indicates that the antiferromagnetic-to-paramagnetic transition is less cooperative and spread over a larger temperature region than for $Fe_{0.9379}O$. The increasing temperature of the heat-capacity maximum with increasing oxygen content agrees qualitatively with the results by Koch and Fine[69] and by Seehara and Srinivasan.[70] According to McCammon[71] the minimum Néel temperature is at 192 K for $Fe_{0.952}O$ and rises to 202 K for $Fe_{0.98}O$.

The molar heat capacities of decomposed $Fe_{0.9254}O$ at $T = 815.42$ K and 839.87 K, and of partly and fully recombined wüstite above, are shown in figure 4. The integrated molar functions are given in table 5. In view of the absence of heat-

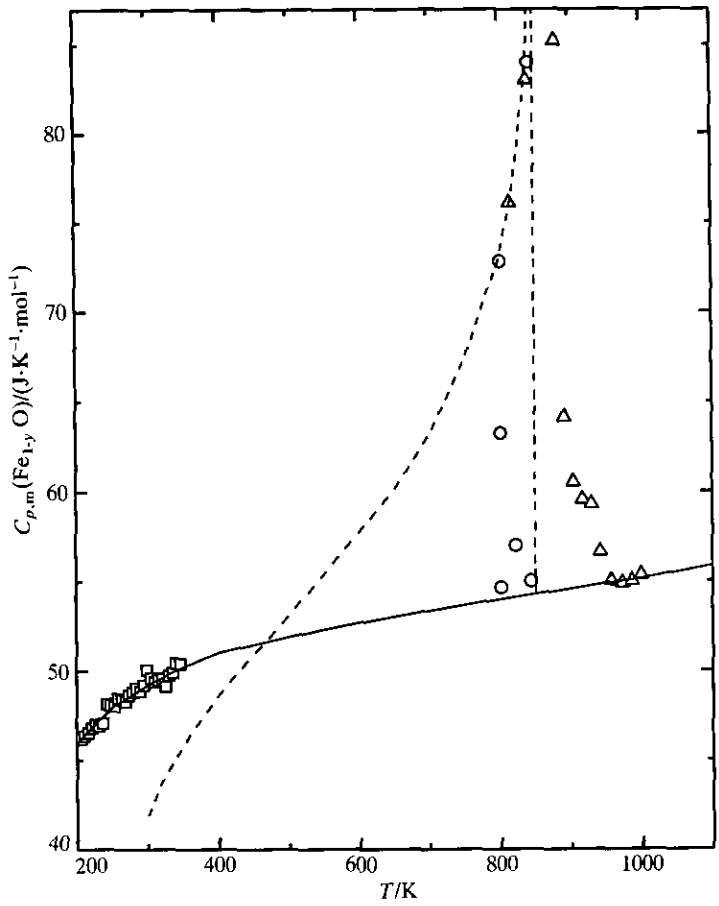

FIGURE 4. Molar heat capacity of $Fe_{0.9254}O$. □, UofM results on quenched wüstite; △, UofO results on decomposed wüstite in the region $T = 800$ K to 850 K and of recombining wüstite above; ———, present equation for wüstite; ○, rising molar heat capacity of supercooled wüstite, $(1/1.92)Fe_{0.92}O$, as result of decomposition treatments in the $T \approx 800$ K to 825 K region, see text.

capacity measurements on pure wüstite from $T = 346.71$ K to 957.08 K the bridging across the metastable wüstite region is rather uncertain, but is fitted with the 4-parameter equation:

$$C_{p,m}/(J\cdot K^{-1}\cdot mol^{-1}) = 50.804 + 4.16562\cdot 10^{-3}(T/K) - 248.1707\cdot 10^{3}(K/T)^2 + 451.70487\cdot 10^{-12}(T/K)^3.$$

The resulting curve is shown in figure 4 also.

The $Fe_{0.9427}O$ sample was not measured over the low-temperature region because of its proximity to $Fe_{0.947}O$, but three results were obtained from $T = 938.76$ K to 964.54 K. They are intermediate between those for $Fe_{0.9379}O$, and the ones for $Fe_{0.947}O$ by Coughlin *et al.*,[55] and show slightly rising molar heat-capacities for $\{1/(2-y)\}Fe_{1-y}O$ with decreasing y at constant T in this region.

In order to estimate the stability of wüstite as function of composition and of temperature, approximate values over a wider composition range are needed. Here we are confronted with the seemingly peculiar trend that the approach to 1–1 stoichiometry of $Fe_{1-y}O$ results in lower molar heat capacity in the $T = 300$ K region than for the iron-deficient samples, while the opposite normal trend prevails in the $T = 900$ K to 1000 K region.

If one tries to estimate a non-magnetic reference molar heat capacity for $Fe_{0.947}O$ by bridging the heat capacity values evenly across the $T = 130$ K to 220 K region only a small fraction of the expected molar magnetic entropy: $\Delta_{trs}S^\circ_m = 0.947 \cdot R \cdot \ln 5 = 12.7\,J \cdot K^{-1} \cdot mol^{-1}$, is accounted for. On comparison with MnO and NiO the decaying molar magnetic heat-capacity contribution appears to be about $5\,J \cdot K^{-1} \cdot mol^{-1}$ at $T = 300$ K, which is indicative of a residual molar magnetic-spin-ordering entropy of about $2.5\,J \cdot K^{-1} \cdot mol^{-1}$. Thus, the molar magnetic entropy acquired by $Fe_{0.947}O$ at $T = 300$ K is about $10\,J \cdot K^{-1} \cdot mol^{-1}$, or about (1/4) of the lattice entropy. The detailed way in which it is acquired profoundly influences the resulting molar heat capacity of wüstite in the $T = 150$ K to 350 K region. Although relatively concentrated for $Fe_{0.947}O$ compared with the present samples, the cooperative nature of the transition presumably increases as the stoichiometric FeO composition is approached. The rising cooperation presumably contributes to the decreasing molar heat capacity for $\{1/(2-y)\}Fe_{1-y}O$ with increasing mole ratio $n(Fe)/n(O)$ at constant T in the post-transitional region up to $T \approx 350$ K.

In considering the molar heat capacity and entropy values at $T \approx 300$ K it should be noted that the molar volume of the $Fe_{1-y}O$ phase is approximately constant for $\{1/(2-y)\}Fe_{1-y}O$, *i.e.* 6.21 $cm^3 \cdot mol^{-1}$ for $(1/1.9254)Fe_{0.9254}O$ and 6.18 $cm^3 \cdot mol^{-1}$ for $(1/1.947)Fe_{0.947}O$ (values derived from X-ray results on quenched samples, see below). Thus, the molar lattice entropy acquired at this temperature would not be expected to differ materially between the three samples.

The $\Delta S^\circ_m(298.15\,K)$ values for $\{1/(2-y)\}Fe_{1-y}O$ are closely concordant for the three samples measured so far: $29.5\,J \cdot K^{-1} \cdot mol^{-1}$ for $(1/1.947)Fe_{0.947}O$ according to Todd and Bonnickson,[54] $29.46\,J \cdot K^{-1} \cdot mol^{-1}$ for $(1/1.9379)Fe_{0.9379}O$, and $29.20\,J \cdot K^{-1} \cdot mol^{-1}$ for $(1/1.9254)Fe_{0.9254}O$. The slight increase in molar entropy with increasing mole ratio $n(Fe)/n(O)$ for our two samples leads us to estimate $\Delta S^\circ_m(298.15\,K) = (61 \pm 1)\,J \cdot K^{-1} \cdot mol^{-1}$ for FeO and $(55 \pm 1)\,J \cdot K^{-1} \cdot mol^{-1}$ for $Fe_{0.90}O$, while Haas[64] derived $63.459\,J \cdot K^{-1} \cdot mol^{-1}$ and $51.987\,J \cdot K^{-1} \cdot mol^{-1}$.

Molar heat capacities for FeO and $Fe_{0.90}O$ in the range $T = 300$ K to 1300 K were estimated by comparison with those for $Fe_{0.947}O$ by Coughlin *et al.*[55] and the trends shown by the present results for $Fe_{0.9379}O$ and $Fe_{0.9254}O$. The resulting values for the molar thermodynamic functions are listed in table 6. They vary considerably from those from the network evaluation by Haas[64] which included the drop-calorimetric results by Rogez *et al.*[60] We do not consider the increasing trend deduced by the latter authors for the molar enthalpy increments $\Delta^{1179\,K}_{299\,K}H^\circ_m$ as trustworthy for $Fe_{1-y}O$ with decreasing number of iron atoms, because of the large scatter in the results, and since the molar enthalpy increment determined by Coughlin *et al.*[55] for $Fe_{0.947}O$ was about 4 per cent higher than the result by Rogez

TABLE 6. Estimated thermodynamic properties of FeO and $Fe_{0.90}O$, $R = 8.3145\ J \cdot K^{-1} \cdot mol^{-1}$

$\frac{T}{K}$	$\frac{C_{p,m}}{R}$	$\frac{\Delta^T_{298.15K}H^\circ_m}{R \cdot K}$	$\frac{\Delta^T_0 S^\circ_m}{R}$	$\frac{\Phi^\circ_m + \Delta^{298.15K}_0 H^\circ_m/T}{R}$	$\frac{C_{p,m}}{R}$	$\frac{\Delta^T_{298.15K}H^\circ_m}{R \cdot K}$	$\frac{\Delta^T_0 S^\circ_m}{R}$	$\frac{\Phi^\circ_m + \Delta^{298.15K}_0 H^\circ_m/T}{R}$
		$M(FeO) = 71.846\ g \cdot mol^{-1}$				$M(Fe_{0.90}O) = 66.262\ g \cdot mol^{-1}$		
298.15	5.730	0	7.337	7.337	5.909	0	6.615	6.615
300	5.739	10.609	7.372	7.337	5.913	10.935	6.652	6.615
350	5.943	302.93	8.273	7.407	6.010	309.17	7.571	6.688
400	6.095	604.04	9.077	7.567	6.077	611.44	8.378	6.849
450	6.218	911.98	9.802	7.775	6.127	916.60	9.097	7.060
500	6.323	1225.6	10.463	8.012	6.168	1224.0	9.745	7.297
550	6.415	1544.1	11.070	8.262	6.203	1533.3	10.334	7.546
600	6.498	1866.9	11.632	8.520	6.234	1844.2	10.875	7.801
650	6.576	2193.8	12.155	8.780	6.263	2156.7	11.375	8.507
700	6.648	2524.4	12.645	9.039	6.292	2470.6	11.841	8.311
750	6.718	2858.6	13.106	9.294	6.320	2785.6	12.276	8.561
800	6.784	3196.1	13.541	9.546	6.349	3102.6	12.684	8.806
850	6.848	3536.9	13.955	9.794	6.379	3420.8	13.070	9.046
900	6.910	3880.9	14.348	10.036	6.410	3740.5	13.436	9.280
950	6.970	4227.9	14.723	10.273	6.443	4061.8	13.776	9.508
1000	7.029	4577.9	15.082	10.504	6.478	4384.8	14.115	9.730
1050	7.086	4930.8	15.427	10.731	6.514	4709.6	14.431	9.946
1100	7.142	5286.5	15.758	10.952	6.553	5036.3	14.735	10.157
1150	7.197	5645.0	16.076	11.168	6.595	5365.0	15.028	10.362
1200	7.251	6006.2	16.384	11.378	6.639	5695.8	15.309	10.563
1250	7.303	6370.1	16.681	11.585	6.686	6029.0	15.581	10.758

et al.[60] Furthermore, it becomes increasingly more difficult to retain the wüstite phase on quenching when the samples become more oxygen rich. Thus, the presence of one tenth decomposed $Fe_{0.90}O$, as ($0.006Fe + 0.025Fe_3O_4$), would require an additional enthalpy increment on heating from $T = 299$ K and recombination in the calorimeter of $1.2\ kJ \cdot mol^{-1}$. The electrical conductivity results by Rogez *et al.*[60] substantiate that considerable disproportionation takes place for the two most oxygen-rich samples when quenched. Enthalpy titrations across the wüstite field at $T = 1073$ K by Gerdanian and Dodé,[72] and at 1348 K by Marucco *et al.*[73] appear to support the present selection, see below.

THE FORMATION OF WÜSTITE FROM Fe AND Fe_3O_4

The molar heat-capacity results of the decomposed wüstite with overall composition $Fe_{0.9427}O$ are given in table 3 above. Further details about the recombination reaction are found in table 7. Considerable uncertainty is attached to the temperature of eutectoid recombination of iron and magnetite to form wüstite. Heat-capacity determinations on $Fe_{0.9427}O$ were, therefore, carried out with several small energy inputs as the reaction temperature was approached in order to find the starting temperature of the eutectoid enthalpy absorption. The heat-capacity maximum, due to the ferrimagnetic transition in Fe_3O_4 at $T = 848.5$ K,[74] was passed without extra-instrumental change in drift rate of the calorimeter, as was also the next determination, which brought the calorimeter temperature up to 853.7 K.

TABLE 7. Enthalpy of reaction for $x\mathrm{Fe}+0.25\mathrm{Fe_3O_4} = \mathrm{Fe_{(0.75+x)}O}$, where $(0.75+x) = 0.9427$, 0.9379, and 0.9254

$\langle T\rangle$/K	$C_{p,m}/R$	ΔT/K	$\Delta H_m^\circ/R\cdot\mathrm{K}$	$\Delta_{n.t.}H_m^\circ/R\cdot\mathrm{K}$	$\Delta_t H_m^\circ/R\cdot\mathrm{K}$	t_{stab}/min	T_{fin}/K
			$M(\mathrm{Fe_{0.9427}O}) = 68.646\ \mathrm{g\cdot mol^{-1}}$				
853.762	348.67	0.49759	173.55	3.247	170.31	2807	854.010
854.413	184.02	0.80479	148.06	5.412	142.64	1255	854.815
858.786	89.688	7.9417	712.26	52.799	659.46	1433	862.756
871.078	11.195	16.643	186.30	110.89	75.411	4352	879.399
					1047.8		
Phase reaction at $T = 850$ K to 853.5 K					9.5		
Phase reaction at $T = 879.4$ K to 932 K					12.4		
					1069.7 ± 70		
			$M(\mathrm{Fe_{0.9379}O}) = 68.378\ \mathrm{g\cdot mol^{-1}}$				
851.670	83.025	12.990	1078.5	104.76	973.73	1178	858.164
862.944	11.673	9.5581	111.61	63.384	48.230	304	867.722
871.403	11.822	7.3601	86.957	48.831	38.127	1119	875.083
880.904	7.892	11.643	91.889	77.215	14.673	175	886.725
892.568	7.351	11.985	88.160	79.501	8.660	175	898.410
					1083.4 ± 20		
No phase reaction at $T > 898.4$ K							
			$M(\mathrm{Fe_{0.9254}O}) = 67.680\ \mathrm{g\cdot mol^{-1}}$				
853.222	58.116	16.172	939.81	125.57	814.25	895	861.307
864.835	20.458	7.0552	144.33	46.185	98.143	726	868.362
871.627	21.950	6.5291	143.37	42.697	100.67	1525	874.891
880.252	10.245	10.721	109.81	70.240	39.570	596	885.612
891.725	7.714	12.224	94.294	79.861	14.433	104	897.836
					1067.0		
Phase reaction at $T = 897.8$ K to 948.6 K					25.1		
					1092.2 ± 30		

The following energy input raised the temperature to about 860 K shortly after the input, but with a drift rate of $-2\cdot10^{-4}\ \mathrm{K\cdot s^{-1}}$ after 1 h, or 15 times that of the previous determination. After a waiting time of 47 h the calorimeter temperature was 854.1 K, with an acceptable drift rate of $-1.3\cdot10^{-5}\ \mathrm{K\cdot s^{-1}}$. The transformation temperature was taken to be about 854 K, and additional energy introduced. Equilibration times of 45 h were needed for absorption of most of the enthalpy during the next two inputs, while an additional time of 73 h brought out 7 per cent more. Presumably more of the enthalpy would have been absorbed at lower temperatures if the equilibration period had been extended to about 20 d instead of 6.8 d, but with detrimental effect on the accuracy of the transitional enthalpy. For this sample some phase reaction occurred all the way up to $T = 932$ K, which indicates that the composition of the sample is probably on the iron-rich side of the eutectoid composition.

For $\mathrm{Fe_{0.9379}O}$, measurements were started at ambient temperature, see table 3, Series I, and figure 3. The mixture of Fe and $\mathrm{Fe_3O_4}$ has lower molar heat capacity than quenched wüstite in the region $T = 300$ K to 450 K. It rises considerably above

that of metastable wüstite with further increase in temperature due to magnetic disordering in ferrimagnetic Fe_3O_4 on its approach to the Curie temperature.

The molar heat capacity calculated from the above mechanical mixture of Fe and Fe_3O_4 is shown as a dashed line in figure 3 for $Fe_{0.9379}O$. It is about 1.2 per cent higher than the experimental results for decomposed $Fe_{0.9379}O$ over the region $T = 320$ K to 420 K, and agrees even better over the range 791.94 K to 840.05 K.

As the eutectoid temperature had already been determined for $Fe_{0.9427}O$, it was decided to bridge the eutectoid region with one large energy input. It turned out, however, that 1 d of equilibration time was not sufficient to complete the reaction. An additional 5 h of equilibration in the $T = 867.7$ K region still left the reaction incomplete, but one additional energy input with 1 d of equilibration at $T = 875$ K made the reaction 98 per cent complete. No phase reaction was observed at $T > 898.4$ K after 2.0 d total equilibration time at $T > 854$ K, indicating that $Fe_{0.9379}O$ has a composition closer to the eutectoid than does $Fe_{0.9427}O$.

Finally, for $Fe_{0.9254}O$ a large energy input was given at $T \approx 845$ K. It resulted in a relatively smaller enthalpy increase than that for $Fe_{0.9379}O$. Comparatively more enthalpy was acquired above $T = 868$ K, and with longer equilibration times. Thus, there seem to be further kinetic hindrances to equilibration, and/or slow phase reactions taking place at temperatures up to 948 K. Hence, $Fe_{0.9254}O$ appears to be further away from the eutectoid composition than $Fe_{0.9379}O$, and on the Fe_3O_4 side.

The lattice constants of wüstites quenched from different temperatures are of further aid in locating the composition of the eutectoid. This was demonstrated by Jette and Foote,[1,2] in their pioneering work, which showed that wüstites quenched from $T = 880$ K had lattice constant $a = 430.4$ pm in equilibrium with iron ($x_O = 0.5169$) and $a = 429.7$ pm in equilibrium with magnetite ($x_O = 0.5199$).† Numerous authors have since reported lattice constants and compositions of quenched wüstites. Some of the more accurate results (compare references 3, 4, 13–15, 70, 75, and 76) are shown in figure 5. The uncertainty is caused mainly by inaccuracy of the oxygen content of the wüstite, which in many cases was indirectly determined.

A linear extrapolation of the curve towards stoichiometric FeO gives lattice constants in the range $a = 433.0$ pm to 433.3 pm. Wüstite samples showing lattice constants in this range were obtained in the present study as result of furnace cooling, and/or incomplete equilibration; see table 1.

If one assumes that the wüstite composition in equilibrium with magnetite changes about twice as much with temperature towards the eutectoid composition as the iron-side boundary, the quenched eutectoid should show $a = 430.1$ pm according to the results by Jette and Foote[1,2] as well as those obtained here. From the results shown in figure 5, this lattice-constant value corresponds to a eutectoid wüstite composition close to $Fe_{0.932}O$. (This is consistent with the $Fe_{0.9379}O$ sample being closest to the eutectoid composition among the three samples prepared here.) The non-transitional $\Delta_{n.t.}H^\circ_m$ in table 7 is derived on the assumption that the wüstite formation temperature is 850 K, see below. For $Fe_{0.9427}O$ the uncertainty is

† The values, based on a(NaCl, 293 K) = "5.6280 A", were converted to a/pm using the factor 100.22.

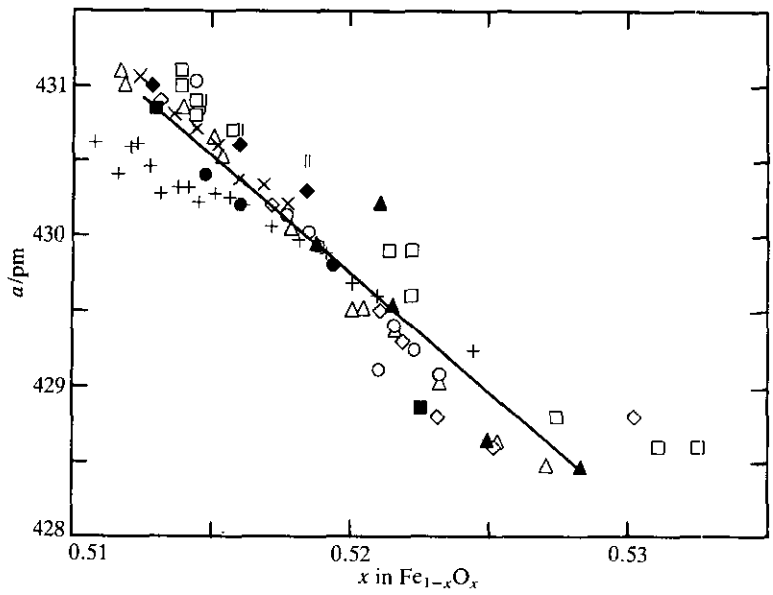

FIGURE 5. Lattice constants of quenched wüstites at ambient temperature. ○, Jette and Foote;[1,2] △, Levin and Wagner;[9] □, Marion;[3] ◇, Touzelin;[13] +, Carel,[75] quenched from $T = 1613$ K; ×, Carel,[75] quenched from $T = 1473$ K; —, equation by Fuji and Meussner;[76] ▲, Bredesen and Kofstad;[15] ■, Foster and Welch;[4] ‖, Battle and Cheetham;[14] ◆, Seehra and Srinivasan;[70] ●, present results for $Fe_{0.9427}O$, $Fe_{0.9379}O$, and $Fe_{0.9254}O$ quenched from $T = 870$ K.

estimated to be about 500 $J \cdot mol^{-1}$ due to the extremely long equilibration (+phase reaction) time of 7.1 d. The determinations for $Fe_{0.9379}O$ and $Fe_{0.9254}O$ are considerably more accurate because of the shorter equilibration time (2.1 d and 3.0 d).

According to the X-ray results the eutectoid wüstite composition is $Fe_{0.932}O$. It is just in the middle between those of our $Fe_{0.9379}O$ and $Fe_{0.9254}O$ samples. If we take the mean molar reaction enthalpy: (9045 ± 300) $J \cdot mol^{-1}$, to be acquired at $T =$ 850 K, the molar reaction entropy is (10.6 ± 0.4) $J \cdot K^{-1} \cdot mol^{-1}$ for

$$0.1817Fe + (1/4)Fe_3O_4 = Fe_{0.9317}O.$$

In the absence of unaccounted structural or magnetic entropy at $T \to 0$, the molar entropy of the reaction should match the molar entropy difference of product minus reactants.

In order to determine the reaction-entropy values, thermodynamic results for Fe and Fe_3O_4 are also needed. Those for Fe are taken from the recent compilation by Haas and Chase,[77] while those for Fe_3O_4 were revaluated here; see appendix.

The resulting molar entropy difference is $(111.1 - 88.8 - 10.8)$ $J \cdot K^{-1} \cdot mol^{-1} =$ (11.5 ± 0.3) $J \cdot K^{-1} \cdot mol^{-1}$. If the reaction should have occurred at $T = 825$ K the non-transitional molar enthalpy would have been 770 $J \cdot mol^{-1}$ less. The molar transitional entropy thereby increases to 11.7 $J \cdot K^{-1} \cdot mol^{-1}$, and the calculated molar entropy difference likewise to $(109.9 - 85.6 - 10.9)$ $J \cdot K^{-1} \cdot mol^{-1} =$

12.5 $J \cdot K^{-1} \cdot mol^{-1}$. The disagreement (0.8 or 0.9) $J \cdot K^{-1} \cdot mol^{-1}$ is somewhat larger than expected in the absence of structural or magnetic entropy at $T \to 0$ in Fe_3O_4 and needs further scrutiny.

In view of the large spread in the eutectoid temperature determinations of wüstite among different authors (about 100 K, with the majority of values from $T = 833$ K to 853 K) some additional experiments were carried out on an earlier sample of comparable purity and composition $Fe_{0.92}O$. (The greater parts of the present samples had in the meantime been used in the chemical analyses). Heating this $Fe_{0.92}O$ in the calorimeter to $T = 875$ K with subsequent cooling to $T = 825$ K during 3 h resulted in a molar heat capacity of about 57 $J \cdot K^{-1} \cdot mol^{-1}$, which indicates that wüstite is the major phase in the sample, see figure 4. The temperature was then kept at 813 K for 3 d with major decomposition as result. The recombination started after an energy input which brought the sample temperature to 848.2 K before a strong negative drift took it down to 843.7 K after 18 h. About 60 per cent of wüstite recombination enthalpy absorption occurred during further energy inputs up to $T = 853.8$ K. A new decomposition was tried with about 10 h of tempering at $T = 816$ K. The molar heat capacity then became 84 $J \cdot K^{-1} \cdot mol^{-1}$ at $T = 844$ K, indicating practically complete disproportionation of the wüstite to $(Fe + Fe_3O_4)$. Heating at $T = 900$ K for 2 d and cooling to $T = 839$ K gave $C_{p,m} =$ 55 $J \cdot K^{-1} \cdot mol^{-1}$ at $T = 844$ K. Further cooling to $T = 826$ K (2 d), 817.5 K (1 d), and to $T = 798$ K overnight all resulted in values approximately as above ($C_{p,m} \approx$ 54.5 $J \cdot K^{-1} \cdot mol^{-1}$ at $T \approx 800$ K). After 1 d more at $T = 798$ K, $C_{p,m} =$ 63.2 $J \cdot K^{-1} \cdot mol^{-1}$, while 3 d plus 3 d more gave $C_{p,m} = 72.8$ $J \cdot K^{-1} \cdot mol^{-1}$ at $T = 801.8$ K and 800.5 K, respectively. These points are plotted on figure 4 and indicate practically complete disproportionation of $Fe_{0.92}O$ to Fe and Fe_3O_4. Thus, considerable supercooling seems to be needed for the disproportionation reaction to take place after complete removal of Fe and Fe_3O_4 from the wüstite at $T = 900$ K, while the partly decomposed sample continued to decompose comparatively quickly at $T = 816$ K.

In addition to the influence of impurities on the location of the eutectoid temperature, the lower values observed on cooling might be related to the types of nuclei formed. Thus, on the magnetite side the secondary precipitating nuclei might contain iron in the paramagnetic state instead of the ferro- or ferri-magnetic states of the larger aggregates, and on the iron side the secondary precipitating spinel-type nuclei might have approximately random instead of about 50 per cent inverse cation distribution.

THERMODYNAMICS OF FORMATION OF WÜSTITE, AND THE PHASE FIELD OF WÜSTITE FOR $T < 1273$ K

In the recent thermodynamic study by Haas[64] the phase boundaries of wüstite were found to approach the composition $Fe_{0.917}O$ at the eutectoid temperature 839.15 K. The eutectic temperature represents a reasonable value within the broad range of observations, while the composition is at variance with many investigations and evaluations which indicate a eutectic composition near $Fe_{0.945}O$.[48-53]

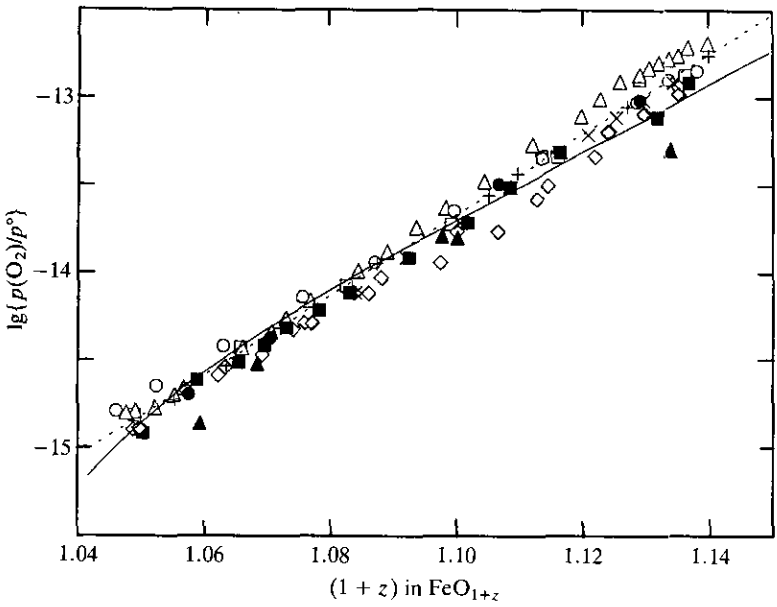

FIGURE 6. Plot of $\lg\{p(O_2)/p^\circ\}$ against $(1+z)$ for wüstites FeO_{1+z} at $T \approx 1270$ K. ▲, Marion;[3] △, Ackermann and Sandford;[78] □, Vallet and Raccah;[28] ◇, Levin and Wagner;[9] ×, Swaroop and Wagner;[20] ■, Bransky and Hed;[79] ●, Riecke and Bohnenkamp;[80] ○, Touzelin;[13] +, Löhberg and Stannek;[62] ———, Sundman;[53] – – –, Haas.[64]

For the present investigation to aid in the solution of the discrepancy, the experimental results needed to be linked to the formation functions of the wüstite phase at temperatures where they have been determined with sufficient accuracy as functions of composition. The closest temperatures for which the oxygen partial pressures have been measured with some accuracy are near $T = 1070$ K. Results around $T = 1270$ K are more accurate, more plentiful, and cover a wider composition range. At even higher temperatures side reactions, including solid solubility, play increasingly larger roles.

In view of the apparent absence of sizeable energetic transitions for $Fe_{0.947}O$ in the region $T = 1000$ K to 1270 K,[55] and the consistent behavior of our samples in the $T = 940$ K to 1000 K region, we feel that the extrapolation of the present results can be made relatively safely. A further check on the validity of the extrapolation is obtained by observing the fit obtained with existing experimental results at $T < 1270$ K; see below.

In figure 6 are plotted literature values for O_2 pressures in the $T = 1270$ K region as function of wüstite composition as FeO_{1+z}. There seem to be two different trends, that with a steeper slope, represented by the results of Ackermann and Sandford,[78] while the more gentle slope is characteristic of the results by Marion,[3] by Vallet and Raccah,[28] by Levin and Wagner,[9] by Swaroop and Wagner,[20] by Bransky and Hed,[79] by Riecke and Bohnenkamp,[80] by Touzelin,[13] and by Löhberg and Stanneck.[62] The results by Himmel *et al.*,[81] and by Giddings[82] are at

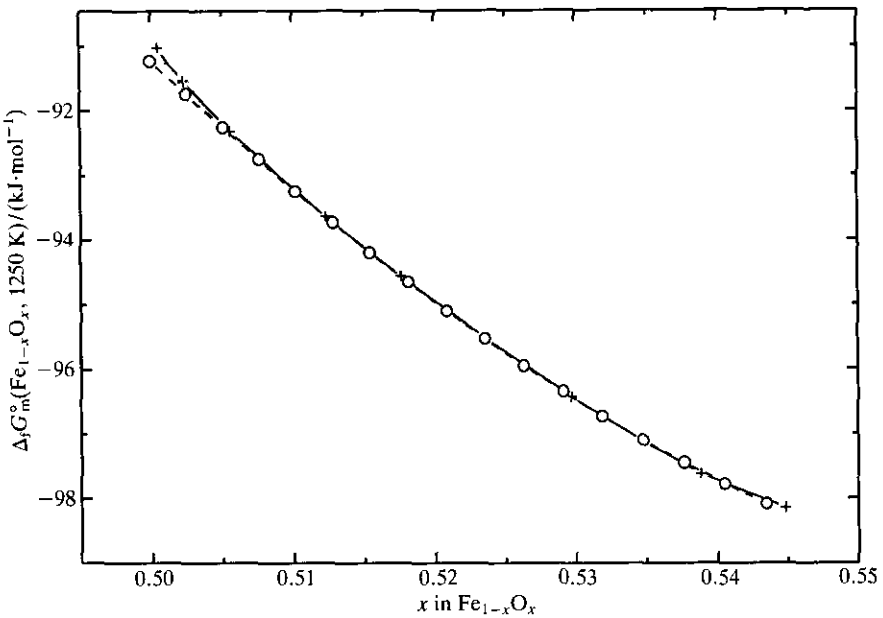

FIGURE 7. Standard molar Gibbs free energy of formation of wüstite, $Fe_{1-x}O_x$, at $T = 1250$ K. +, Sundman;[53] ○, Haas.[64]

temperatures somewhat too far away from 1273 K to be considered; while those by Hauffe and Pfeiffer,[83] by Janowsky *et al.*,[84] and by Myers and Eugster[85] are not sufficiently accurate to warrant consideration.

The linear equation used by Haas[64] for $\lg\{p(O_2)/p^\circ\}$ against excess oxygen for FeO_{1+z} is also shown in figure 6. It was chosen in the evaluation of the voluminous literature pertaining to the thermodynamics of (iron + silicon + oxygen). Another more limited revaluation of (iron + oxygen) by Sundman[53] also results in a reasonable fit to the selected values in figure 6 inside the stable homogeneity range of the wüstite phase at $T = 1270$ K. The functional behavior of the oxygen pressure near stoichiometric FeO is profoundly influenced by Sundman's use of the compound-energy model by Hillert *et al.*,[86] which contains a structural randomization term for Fe^{2+}, Fe^{3+}, and vacancies in $Fe_{1-y}O$. The available evidence on cluster formation in wüstite contradicts this model and points towards a more modest structural randomization even at $T = 1270$ K. Furthermore, close to stoichiometry some other defect process is of importance, which prevents the chemical potential of O_2 from approaching $-\infty$.

In the absence of information about the energetics of such processes in $Fe_{1-y}O$, we are presently basing our analysis on the results of Sundman's[53] and Haas's[64] evaluations of the standard molar Gibbs free energy of formation values for $Fe_{1-x}O_x$ at $T = 1250$ K. The differences between them become important as the $Fe_{1-y}O$ phase approaches stoichiometry ($y = 0$, or $x = \frac{1}{2}$), see figure 7. For (1/2)FeO the $\Delta_f G^\circ_m(1250\ K) = -91231\ J \cdot mol^{-1}$ was taken from Haas[64] alone, while for the other

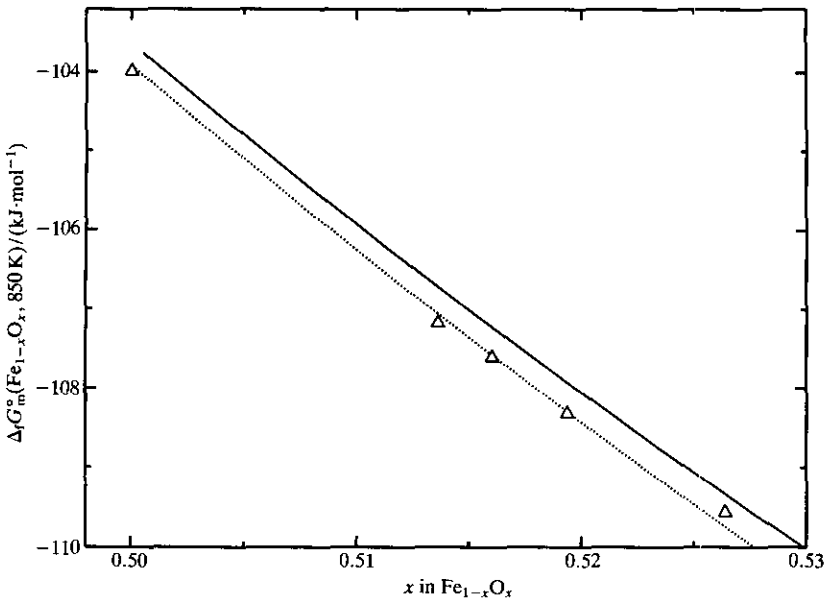

FIGURE 8. Standard molar Gibbs free energy of formation of wüstite, $Fe_{1-x}O_x$, at $T = 850$ K. ———, Sundman;[53] ···, Haas;[64] △, present evaluation, transposed from $T = 1250$ K.

compositions the practically coinciding values by Haas and by Sundman were used. The treatments by Haas[64] and by Sundman[53] give significantly different $\Delta_f G^\circ_m$s for the $Fe_{1-y}O$ phase also when the eutectoid temperature is approached. The curves for $T = 850$ K are shown in figure 8, together with values for (1/2)FeO, (1/1.947)$Fe_{0.947}O$, (1/1.9379)$Fe_{0.9379}O$, (1/1.9254)$Fe_{0.9254}O$, and (1/1.90)$Fe_{0.90}O$. The temperature dependence of $\Delta_f G^\circ_m$ was obtained with values for the oxides from tables 5 and 6, except for (1/1.947)$Fe_{0.947}O$, where we relied on the results by Coughlin *et al.*[55] As seen from figure 8 the formation values are considerably closer to those derived by Haas[64] than to those derived by Sundman.[53] The presently derived values do, however, become more negative than those by Haas when stoichiometry is approached, and favor a slope closer to that obtained by Sundman.[53]

In view of these differences it seemed of interest to see how the molar enthalpies of formation varied with composition in the different treatments. Here we have chosen the temperatures 1075 K and 1350 K, which correspond closely to the temperatures at which Gerdanian and Dodé[72] and Marucco *et al.*[73] performed enthalpy titrations through the wüstite phase region.

The former results are shown in figure 9 for $Fe_{1-y}O$, taking $\Delta_f H^\circ_m(Fe_{0.9254}O, 1075\,K) = -264.3\,kJ\cdot mol^{-1}$ as the practically coinciding result obtained by Gerdanian and Dodé,[72] by Sundman,[54] and by us. The curve representing Haas's[64] values is not far from linear. The value derived for FeO here supports that result. When fitting the present results and those from Gerdanian and Dodé[72] by a

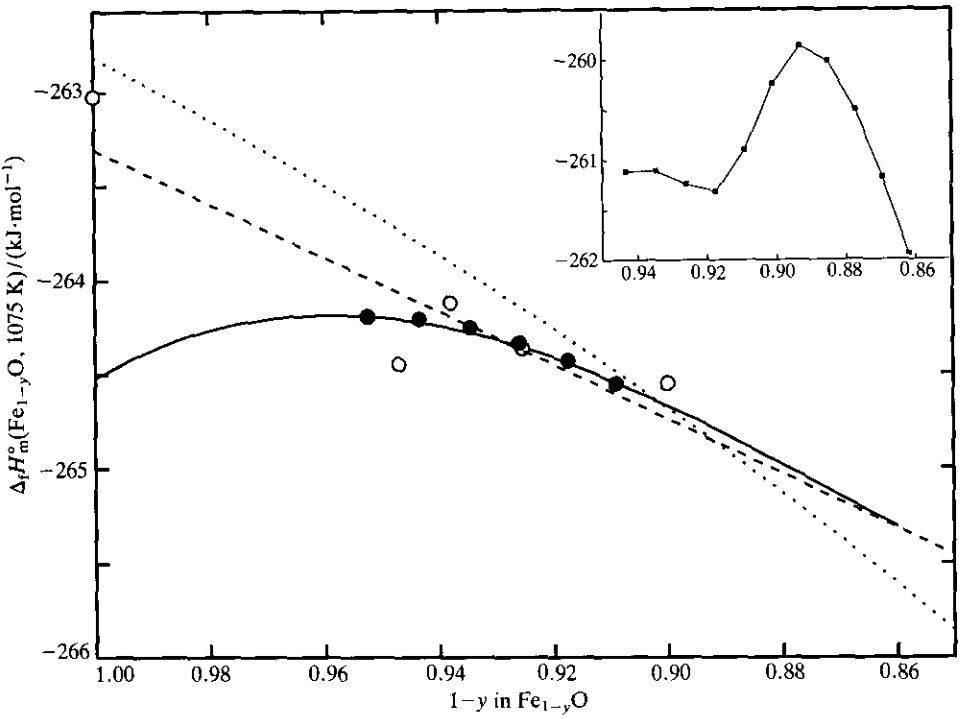

FIGURE 9. *Molar enthalpy of formation of wüstite, as* $Fe_{1-y}O$, *at* $T = 1075$ K. ●, *Enthalpy-titration* results by Gerdanian and Dodé,[72] relative to $\Delta_f H^\circ_m(Fe_{0.9254}O) = -264.3\ kJ\cdot mol^{-1}$; ○, present evaluation; – – –, linear regression of the combined results; ———, Sundman;[53] ···, Haas;[64] insert, evaluation by Spencer and Kubaschewski[49] in the region $T = 840$ K to 1680 K.

straight line we obtain $\Delta_f H^\circ_m(FeO, 1075\ K) = -263.3\ kJ\cdot mol^{-1}$. An insert shows results of the evaluation by Spencer and Kubaschewski.[49] They represent average values for each composition over the region $T = 840$ K to 1680 K.

The titration results by Marucco *et al.*[73] at 1348 K are shown in integrated form in figure 10. The reference value for $(1-y) = 0.947$ is transposed here from $T = 1075$ K to 1350 K, using the enthalpy increment for $Fe_{0.947}O$ Coughlin *et al.*[55] The evaluations by Haas and by Sundman show some curvature, while those by Marucco *et al.*[73] and the present one come close to a straight-line extrapolation and give $\Delta_f H^\circ_m(FeO, 1350\ K) = -263.1\ kJ\cdot mol^{-1}$. It should be remarked, however, that extrapolation of the heat capacity of the samples from $T = 1000$ K to 1350 K is somewhat uncertain, considering the many different cluster arrangements which have been reported inside the macroscopic wüstite field. Nevertheless, the close correspondence between the enthalpy titrations and the enthalpy increments assumed here in the region $T = 1000$ K to 1350 K support the assumption that no major transitions occur as a function of composition between the two temperatures, or that enthalpy increments of possible transitions are slow-varying functions of composition.

Finally, the composition limits of the wüstite phase are derived as function of

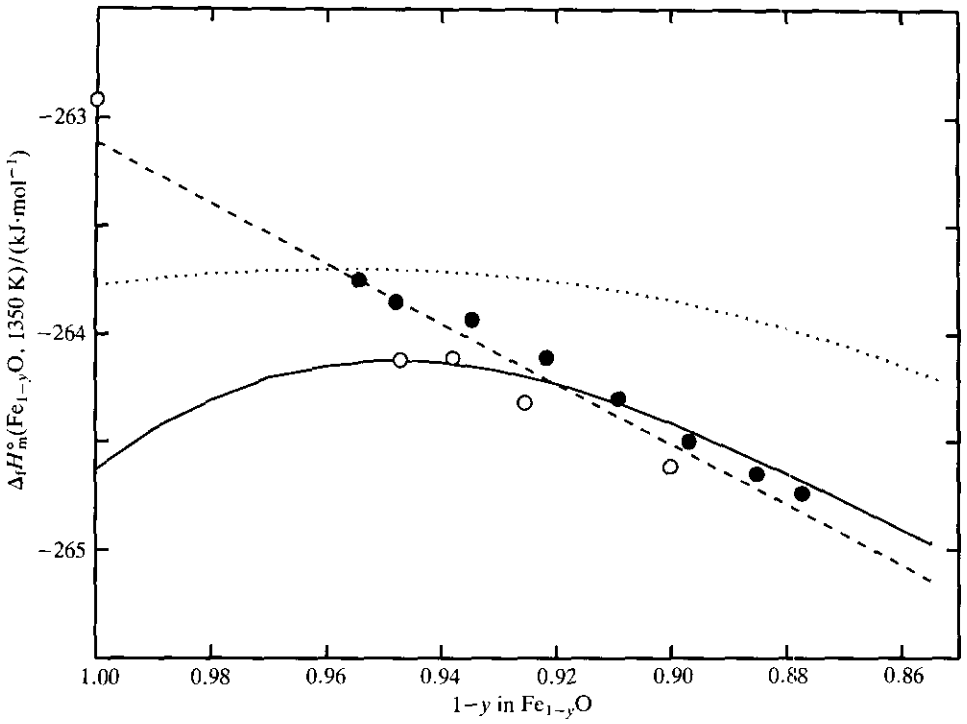

FIGURE 10. Molar enthalpy of formation of wüstite, as $Fe_{1-y}O$, at $T = 1350$ K. ●, Enthalpy-titration results by Marucco *et al.*[73] at $T = 1348$ K, transposed with the enthalpy increment for $Fe_{0.947}O$ by Coughlin *et al.*;[55] ○, present evaluation; – – –, linear regression of the combined results; ———, Sundman;[53] ···, Haas.[64]

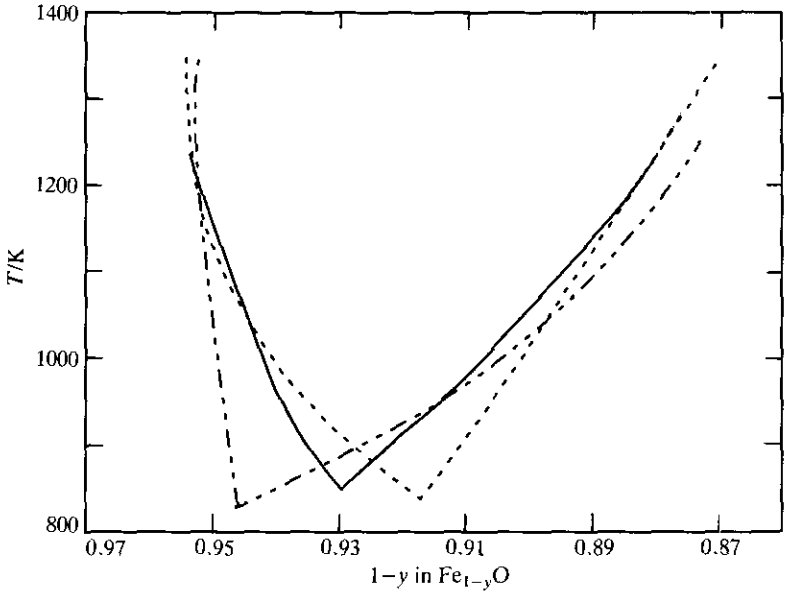

FIGURE 11. Composition limits for the wüstite phase towards Fe (left) and Fe_3O_4 (right). – – –, Haas;[64] – – – –, Sundman;[53] ———, present.

temperature, see figure 11, taking $\Delta_f H^\circ_m(Fe_3O_4, 298.15\ K) = -1115.726\ kJ \cdot mol^{-1}$ from Hemingway.[87] They fall in between those derived by Sundman[53] and by Haas.[64] For iron, negligible solid solubility of oxygen, or FeO, is assumed, while for the $Fe_{3\pm x}O_4$ phase the composition dependence of $\Delta_f G^\circ_m$ reported by Dieckmann[88] is taken into account.

The resulting composition of eutectoid wüstite is $Fe_{0.932\pm0.004}O$ and the decomposition temperature is (847 ± 7) K. The derived composition is intermediate between that by Sundman,[53] $Fe_{0.947}O$, and that by Haas,[64] $Fe_{0.917}O$. In the evaluation by Vallet and Raccah[34] the eutectoid composition was given as $Fe_{0.9345}O$, while in the galvanic-cell study by Barbi[89] it was $Fe_{0.939}O$. The location is a very sensitive function of composition due to the nearly linear $\Delta_f G^\circ_m$ of $Fe_{1-x}O_x$ as function of x in the $T = 850$ K region.

Appendix

The revaluation relies on the adiabatic calorimetry results for Fe_3O_4 by Westrum and Grønvold[90] from $T \approx 5$ K to 350 K, those by Grønvold and Sveen[74] from $T = 300$ K to 1000 K), and those by Bartel and Westrum[91] from $T = 300$ K to 550 K. Recent d.s.c. results by Hemingway[87] from $T = 300$ K to 1000 K are also taken into consideration. Additional results in the low-temperature region[92-95] are not of sufficient accuracy to warrant consideration. For $T > 1000$ K the drop-calorimetric results by Coughlin *et al.*[55] superseded earlier results by Roth and Bertram[96] from $T = 293$ K to 1056 K and by Esser *et al.*[97] from $T = 273$ K to 1273 K. The results by Coughlin *et al.*[55] present a problem in the evaluation in that they agree rather well with the adiabatic calorimetric values up to $T = 800$ K, but deviate negatively at 900 K and 1000 K by 0.3 per cent and 1.3 per cent in $\Delta^T_{298.15\,K}H^\circ_m$. The discrepancy is even more surprising if one considers the enthalpy increments over $\Delta T = 100$ K intervals above 300 K as given in the table by Coughlin *et al.*[55] For $T \leqslant 900$ K they vary from those obtained by Grønvold and Sveen[74] in the range -1.9 per cent to $+1.4$ per cent. Then in the $T = 900$ K to 1000 K interval the difference is -7.6 per cent. We see this sudden drop as related to some quenching effect in the drop-calorimetric experiments. Both the disappearance of ferrimagnetism in Fe_3O_4 at $T \approx 850$ K and the change of the inverse spinel-type structure into the random type are of electronic nature. The latter transition, which is about half complete at $T = 1000$ K according to Wu and Mason[98] might, however, shift the atomic coordinates of the 32 oxygen atoms with coordinates (x, x, x) *etc.*, and $x = 0.3799$† at ambient temperature according to Fleet,[99] to $x = 3/8$, or 0.375, at higher temperatures. Thereby regular coordination is obtained around Fe at the tetrahedral and octahedral centers. If the reverse movement of each O in the right direction on cooling (one out of eight) is not completely cooperative due to rapid cooling, the drop-calorimetric results will be subject to error. The configurational molar entropy increment for Fe_3O_4 due to the change from inverse to random

† Several authors place origin at center $-3m$ (1/8, 1/8, 1/8) in the space group *Fd3m*, No. 227. The suggested change in x is then from 0.2549 to 1/4.

distribution of the Fe atoms is $4.52\ J \cdot K^{-1} \cdot mol^{-1}$. The retention of the remaining $\frac{1}{2}$ of the difference on quenching from $T = 1000$ K, might thus lead to a molar enthalpy loss of $2300\ J \cdot mol^{-1}$ in the drop experiments.

For this reason we use the drop-calorimetric results at $T > 1000$ K in incremental form, which leads to $C_{p,m} = (201 \pm 5)\ J \cdot K^{-1} \cdot mol^{-1}$ in the region $T = 1000$ K to 1500 K.

A large fraction of the heat-capacity determinations by Hemingway[87] by d.s.c. were made on a sample deduced to contain ($0.87Fe_3O_4 + 0.13Fe_2O_3$). The Fe_2O_3 was designated as maghemite (γ-Fe_2O_3), but neither the correction procedure, nor the actually observed heat capacities were reported. (Were they corrected for the presence of maghemite with the results by Grønvold and Samuelsen[100] for α-Fe_2O_3?) The resulting heat capacities for Fe_3O_4 by Hemingway are up to 3 per cent higher in the region $T = 800$ K to 840 K than those obtained by Grønvold and Sveen,[74] and about 3 per cent lower in the range $T = 880$ K to 1000 K.

Hemingway[87] suggested that the sample of Grønvold and Sveen[74] might have contained Fe_2O_3 as an impurity on the basis of "a small rounded heat-capacity anomaly above 900 K" and inferred that a corresponding correction to the heat capacities reported[74] would result in lower heat capacity of Fe_3O_4 at $T > 860$ K ("better agreement among heat capacities measured above 860 K"). The results by Grønvold and Sveen[74] showed only one slightly high value at $T = 933.0$ K, and the overall composition of the Fe_3O_4 sample used was $FeO_{1.334}$. Thus, the presence of some Fe_2O_3 in it would require the presence of some metallic iron or wüstite also. The corresponding correction for the missing amount of Fe_3O_4 would lead to even higher molar heat capacity of Fe_3O_4 in the $T = 800$ K to 900 K region, and for $T > 960$ K.

The molar heat capacity values by Hemingway[87] on the impure material have been used in a least-squares evaluation with weight (1/3) in the region $T = 300$ K to 800 K, while those on single-crystal material have been given weight (1/2); those by Grønvold and Sveen[74] and by Bartel and Westrum[91] have been used with weight 1, while those by Westrum and Grønvold[90] have been used with weight 2 over the region $T = 276.17$ K to 347.94 K.

The d.s.c. results by Hemingway[87] yielded a 3 K lower position of the ferri- to paramagnetic transition maximum temperature, which excludes direct combination with the results by Grønvold and Sveen[74] in the $T = 800$ K to 900 K region. The transformations deduced to exist in $Fe_{3-x}O_4$ at $T = 1040$ K and 1184 K by Vallet and Carel[101] have been disregarded, as they appear to reflect transformations in iron.

In the region $T = 900$ K to 1350 K we have relied on the results by Grønvold and Sveen[74] up to $T = 1044$ K, and those by Hemingway[91] up to $T = 1000$ K with weights as earlier. The results were combined with the average incremental result by Coughlin *et al.*,[55] $C_{p,m} = 201\ J \cdot K^{-1} \cdot mol^{-1}$ at $\Delta T = 25$ K intervals. Results of the integrations are given in table 8.

The work done at the University of Oslo was supported in part by the Norwegian Research Council for Science and the Humanities, whereas the work done at the

TABLE 8. Revaluated thermodynamic properties of Fe_3O_4, $R = 8.3145\ J \cdot K^{-1} \cdot mol^{-1}$

$\frac{T}{K}$	$\frac{C_{p,m}}{R}$	$\frac{\Delta_0^T H_m^\circ}{R \cdot K}$	$\frac{\Delta_0^T S_m^\circ}{R}$	$\frac{\Phi_m^\circ}{R}$	$\frac{T}{K}$	$\frac{C_{p,m}}{R}$	$\frac{\Delta_0^T H_m^\circ}{R \cdot K}$	$\frac{\Delta_0^T S_m^\circ}{R}$	$\frac{\Phi_m^\circ}{R}$
				$M(Fe_3O_4) = 231.539\ g \cdot mol^{-1}$					
298.15	18.181	3011.9	17.578	7.476	850	(36.202	17915.9	42.727	22.791)
300	18.241	3045.6	17.691	7.538	900	26.653	18394.8	44.385	23.946
350	19.760	3996.0	20.618	9.200	950	25.795	19700.7	45.798	25.060
400	21.096	5018.8	23.347	10.800	1000	25.247	20978.2	47.108	26.130
450	22.110	6100.0	25.893	12.337	1050	24.483	22220.3	48.320	27.158
500	23.049	7228.7	28.271	13.813	1100	24.218	23437.0	49.452	28.146
550	24.078	8406.6	30.515	15.230	1150	24.123	24644.9	50.526	29.096
600	25.097	9636.3	32.654	16.594	1200	24.129	25850.9	51.553	30.010
650	26.110	10915.9	34.702	17.909	1250	24.179	27058.5	52.539	30.892
700	27.461	12252.8	36.683	19.179	1300	24.227	28268.8	53.488	31.743
750	29.388	13672.0	38.641	20.411	1350	24.232	29480.5	54.403	32.565
800	31.873	15199.2	40.611	21.612					

University of Michigan was supported in part by the National Science Foundation. The authors wish to thank Dr Bjørn Uhrenius and Sandvik Hard Materials, Sweden for chemical analysis work, and Dr John R. Haas, Jr., U.S. Geological Survey for placing the extensive unpublished material at their disposal. The authors also wish to thank Dr David Garvin at the U.S. National Institute of Standards and Technology for valuable comments and for his continued interest in this study.

REFERENCES

1. Jette, E. R.; Foote, F. *J. Chem. Phys.* **1933,** 1, 29.
2. Jette, E. R.; Foote, F. *Trans. AIME* **1933,** 105, 276.
3. Marion, M. F. *La Documentation Métallurgique* **1955,** 24, 87.
4. Foster, P. K.; Welch, A. J. E. *Trans. Faraday Soc.* **1956,** 52, 1626.
5. Fischer, W. A.; Hoffmann, A. *Archiv Eisenhüttenw.* **1959,** 30, 15.
6. Carel, C. *C.R. Acad. Sci. Paris* **1964,** 258, 1267.
7. Carel, C.; Weigel, D.; Vallet, P. *C.R. Acad. Sci. Paris* **1964,** 258, 6126.
8. Carel, C.; Weigel, D.; Vallet, P. *C.R. Acad. Sci. Paris* **1965,** 260, 4325.
9. Levin, R. L.; Wagner, J. B., Jr. *Trans. AIME* **1966,** 236, 516.
10. Katsura, T.; Iwasaki, B.; Kimura, S.; Akimoto, S. I. *J. Chem. Phys.* **1967,** 47, 4559.
11. Broussard, L. *J. Phys. Chem.* **1969,** 73, 1848.
12. Hentschel, B. *Z. Naturforsch. A* **1970,** 25, 1996.
13. Touzelin, B. *Rev. Intern. Haut. Temp. Réfract.* **1974,** 11, 219; see also *Metalurgia i Odlewenictwo* **1987,** 13, 107.
14. Battle, P. D.; Cheetham, A. K. *J. Phys. C: Solid State Phys.* **1979,** 12, 337.
15. Bredesen, R.; Kofstad, P. *Oxid. Metals* **1991,** 36, 27.
16. Hägg, G. *Trans. AIME* **1933,** 105, 287.
17. Roth, W. L. *Acta Cryst.* **1960,** 13, 140.
18. Manenc, J. *J. Phys. Radium* **1963,** 24, 447.
19. Smuts, J. *J. Iron Steel Inst.* **1966,** 204, 237.
20. Swaroop, B.; Wagner, J. B., Jr. *Trans. AIME* **1967,** 239, 1215.
21. Koch, F.; Cohen, J. B. *Acta Cryst. B* **1969,** 25, 275.
22. Cheetham, A. K.; Fender, B. E. F.; Taylor, R. I. *J. Phys. C* **1971,** 4, 2160.
23. Tchiong Tki Kong; Romanov, A. D.; Shaytovitch, Ya. L. *Vestn. Leningrad Univ. Fiz. Khim.* **1973,** 4, 144.
24. LeCorre, C.; Jeannot, F.; Morniroli, J. P. *C.R. Acad. Sci. Paris C* **1973,** 276, 1335.

25. Andersson, B.; Sletnes, J. O. *Acta Cryst. A* **1977,** 33, 268.
26. Lebreton, C.; Hobbs, L. W. *Rad. Effects* **1983,** 74, 227.
27. Vallet, P.; Kléman, M.; Raccah, P. *C.R. Acad. Sci. Paris* **1963,** 256, 136.
28. Vallet, P.; Raccah, P. *Mém. Sci. Rev. Mét.* **1965,** 62, 1.
29. Manenc, J. *Bull. Soc. Franc. Minéral. Crist.* **1968,** 91, 594.
30. Fender, B. E. F.; Riley, F. D. *J. Phys. Chem. Solids* **1969,** 30, 793.
31. Vallet, P. *C.R. Acad. Sci. Paris C* **1975,** 280, 239.
32. Vallet, P. *C.R. Acad. Sci. Paris C* **1975,** 281, 291.
33. Carel, C.; Gavarri, J. R. *Mater. Res. Bull.* **1976,** 11, 745.
34. Vallet, P.; Carel, C. *Rev. Chim. Minérale* **1986,** 23, 362.
35. Carel, C. *Bull. Soc. Sci. Bretagne* **1987–88,** 59, 111.
36. Vallet, P.; Carel, C. *Bull. Alloy Phase Diagrams* **1989,** 10, 209.
37. Catlow, C. R. A.; Fender, B. E. F. *J. Phys. C* **1975,** 8, 3267.
38. Catlow, R. C. A.; Fender, B. E. F. *J. Phys. Paris* **1977,** Colloque 38, C 7, 67.
39. Catlow, C. R. A.; Stoneham, A. M. *J. Am. Ceram. Soc.* **1981,** 64, 234.
40. Akimitsu, M.; Mizoguchi, T.; Akimitsu, J.; Kimura, S. *J. Phys. Chem. Solids* **1983,** 44, 497.
41. Anderson, A. B.; Grimes, R. W.; Heuer, A. H. *J. Solid State Chem.* **1984,** 55, 353.
42. Gartstein, E.; Mason, T. O. *J. Am. Ceram. Soc.* **1982,** 65, C24.
43. Press, M. R.; Ellis, D. E. *Phys. Rev. B* **1987,** 35, 4438.
44. Bizette, H.; Tsai, B. *C.R. Acad. Sci. Paris* **1943,** 217, 390.
45. Shull, C. G.; Strauser, W. A.; Wollan, E. O. *Phys. Rev.* **1951,** 83, 333.
46. Tombs, N. C.; Rooksby, H. P. *Nature* **1950,** 165, 442.
47. Willis, B. T. M.; Rooksby, H. P. *Acta Cryst.* **1953,** 6, 827.
48. Darken, L. S.; Gurry, R. W. *J. Am. Chem. Soc.* **1945,** 67, 1398.
49. Spencer, P. J.; Kubaschewski, O. *CALPHAD* **1978,** 2, 147.
50. Kubaschewski, O. *Iron–Oxygen, Iron–Binary Phase Diagrams.* Springer Verlag: New York. **1982,** p. 79.
51. Knacke, O. *Ber. Bunsenges. Phys. Chem.* **1983,** 87, 797.
52. Wriedt, H. A. *Bull. Alloy Phase Diagrams* **1991,** 11, 1739.
53. Sundman, B. *J. Phase Equilibria* **1991,** 12, 127.
54. Todd, S. S.; Bonnickson, K. R. *J. Am. Chem. Soc.* **1951,** 73, 3894.
55. Coughlin, J. P.; King, E. G.; Bonnickson, K. R. *J. Am. Chem. Soc.* **1951,** 73, 3891.
56. Millar, R. W. *J. Am. Chem. Soc.* **1929,** 51, 215.
57. White, W. P. *J. Am. Chem. Soc.* **1933,** 55, 1047.
58. Vladimirov, V. P.; Ponomarev, V. D. *Vestnik Akad. Nauk Kazakhskoi SSR* **1959,** 15, 78.
59. Mainard, R.; Boubel, M.; Fousse, H. *C.R. Acad. Sci. Paris B* **1968,** 266, 1299.
60. Rogez, J.; Marucco, J. F.; Castanet, R.; Mathieu, J. C. *Ann. Chim. France* **1982,** 7, 63.
61. Giddings, R. A.; Gordon, R. S. *J. Am. Ceram. Soc.* **1973,** 56, 111.
62. Löhberg, K.; Stannek, W. *Ber. Bunsenges. Phys. Chem.* **1975,** 79, 244.
63. Barbero, J. A.; Blesa, M. A.; Maroto, A. J. G. *Z. phys. Chem. N.F.* **1981,** 124, 139.
64. Haas, J. R., Jr. *Recommended Standard Electrochemical Potentials and Fugacities of Oxygen for the Solid Buffers and Thermodynamic Data in the Systems Iron–Silicon–Oxygen, Nickel–Oxygen, and Copper–Oxygen.* U.S. Geological Survey, Reston, Va. (17 Jan., 1988), personal communication; see also Haas, J. R., Jr.; Hemingway, B. S. *Open File Report 92-267.* U.S. Geological Survey. **1992.**
65. Deslatters, R. D.; Henins, A. *Phys. Rev. Lett.* **1973,** 31, 972.
66. Westrum, E. F., Jr.; Furukawa, G. T.; McCullough, J. P. *Experimental Thermodynamics, Vol. I.* McCullough, J. P.; Scott, D. W.: editors. Butterworths: London. **1968,** p. 133.
67. Westrum, E. F., Jr. *Proceedings NATO Advanced Study Institute on Thermochemistry.* Ribeiro da Silva, A. V.: editor. Reidel: New York. **1984,** p. 745.
68. Grønvold, F. *Acta Chem. Scand.* **1967,** 21, 1695.
69. Koch, F. B.; Fine, M. E. *J. Appl. Phys.* **1967,** 38, 1470.
70. Seehra, M. S.; Srinivasan, G. *J. Phys. C: Solid State Phys.* **1984,** 17, 883.
71. McCammon, C. A. *J. Magnetism Mag. Materials* **1992,** 104–107, 1937.
72. Gerdanian, P.; Dodé, M. *J. Chim. Phys.* **1965,** 62, 1010, 1018.
73. Marucco, J.-F.; Gerdanian, P.; Dodé, M. *J. Chim. Phys.* **1970,** 906, 914.
74. Grønvold, F.; Sveen, A. *J. Chem. Thermodynamics* **1974,** 6, 859.
75. Carel, C. Thesis, Rennes, 1966, according to reference 33.
76. Fujii, C. T.; Meussner, R. A. *Trans. Met. Soc. AIME, Met. Trans.* **1968,** 242, 1259.
77. Haas, J. L., Jr.; Chase, M. *Open File Report, 89-138.* U.S. Geological Survey. **1989.**

78. Ackermann, R. J.; Sandford, R. W., Jr. *Rept. ANL-7250.* U.S. Atomic Energy Comm. **1966.**
79. Bransky, I.; Hed, A. Z. *J. Am. Ceram. Soc.* **1968,** 51, 231.
80. Riecke, E.; Bohnenkamp, K. *Archiv Eisenhüttenw.* **1969,** 40, 717.
81. Himmel, L.; Mehl, R. F.; Birchenall, C. E. *Trans. AIME, J. Metals* **1953,** 5, 827.
82. Giddings, R. A. Thesis, University of Utah, 1972.
83. Hauffe, K.; Pfeiffer, H. *Z. Metallkunde* **1953,** 44, 27.
84. Janowski, J.; Jaworski, M.; Benesch, R. *Archiv. Eisenhüttenw.* **1973,** 44, 721.
85. Myers, J.; Eugster, H. P. *Contrib. Mineral. Petr.* **1983,** 82, 75.
86. Hillert, M.; Jansson, B.; Sundman, B. *Z. Metallk.* **1988,** 79, 81.
87. Hemingway, B. *Am. Mineral.* **1989,** 75, 781.
88. Dieckmann, R. *Ber. Bunsenges. Phys. Chem.* **1982,** 86, 112.
89. Barbi, G. B. *J. Phys. Chem.* **1964,** 68, 2912.
90. Westrum, E. F., Jr.; Grønvold, F. *J. Chem. Thermodynamics* **1969,** 1, 543.
91. Bartel, J. J.; Westrum, E. F., Jr. *J. Chem. Thermodynamics* **1975,** 7, 706.
92. Rigo, M. O.; Mareche, J. F.; Brabers, V. A. M. *Phil. Mag. B* **1983,** 48, 421.
93. Gmelin, E.; Lenge, N.; Kronmüller, H. *Phys. stat. sol. a* **1983,** 79, 465.
94. Gmelin, E.; Lenge, N.; Kronmüller, H. *Phil. Mag. B* **1984,** 50, L41.
95. Shepherd, J. P.; Koenitzer, J. W.; Aragon, R.; Sandberg, C. J.; Honig, J. M. *Phys. Rev. B* **1985,** 31, 1107.
96. Roth, W. A.; Bertram, W. *Z. Elektrochem.* **1929,** 35, 297.
97. Esser, H.; Averdieck, R.; Grass, W. *Arch. Eisenhüttenw.* **1933,** 6, 289.
98. Wu, C. C.; Mason, T. O. *J. Am. Ceram. Soc.* **1981,** 64, 520.
99. Fleet, M. J. *Solid State Chem.* **1986,** 62, 75.
100. Grønvold, F.; Samuelsen, E. J. *J. Phys. Chem. Solids* **1975,** 36, 249.
101. Vallet, P.; Carel, C. *Rév. Chim. Minérale* **1987,** 24, 719.